Nanoscale Design of Pd-based Electrocatalysts for ORR Enhancement in Alkaline Media

Ming Zhou,[†] Jiangna Guo,[‡] and Jiye Fang*[,†]

[†]Department of Chemistry, State University of New York at Binghamton, Binghamton, New York 13902, United States.

[‡]College of Chemistry and Chemical Engineering, Chongqing University, Chongqing 400044, China.

*Corresponding author: E-mail: jfang@binghamton.edu

Abstract

Palladium (Pd)-based electrocatalysts have recently emerged as one class of the foremost promising candidates for the oxygen reduction reaction (ORR) in alkaline media due to their excellent ORR activity and durability and lower costs compared with platinum. Insightful design of Pd-based nano-architectures with optimized active surface sites and maximal intrinsic performance is central to promoting the ORR applications. To further accelerate the sluggish ORR kinetics at the cathode of fuel cells and substantially decrease the overall cost of the electrocatalysts, various strategies including controlled sizes and shapes with selected crystallographic facets, crystal-phase engineering, heteroatom doping, tailored surface strains, and surface engineering by de-alloying, have been extensively developed during the past decade. In this review, we first present a brief introduction to the fundamental ORR mechanisms of Pd-based electrocatalysts in alkaline media, followed by a thorough discussion on various strategies for delicately designing high-performance Pd-based catalysts with corresponding examples. Thereafter, we outline the perspectives and new insights on the challenges and also propose some emerging research directions related to the rational design and controlled synthesis of Pd-based ORR electrocatalysts.

1. Introduction

As key alternative energy conversion technologies for directly converting chemical energy into electrical energy, fuel cells have attracted increasing interest due to their multitudinous advantages including high energy conversion efficiency, environmental benignancy, and high energy density.[1-4] In recent years, considerable efforts have been primarily devoted to investigating the oxygen reduction reaction (ORR) at the cathode, one of the key catalytic reactions in fuel cells.[5-7] Especially, platinum (Pt)-based electrocatalysts set as benchmarks have been well-documented to possess excellent ORR activity and stability in practical fuel cells.[8-10] Owing to the sluggish ORR kinetics derived from the multielectron and multistep process, however, a significant amount of Pt-based electrocatalysts is often required, resulting in the higher overall cost for a fuel cell device.[11-13] It has also been confirmed that Pt-based electrocatalysts exhibit poor methanol tolerance and low resistance to impurities, such as chloride ions and CO on electrolytes, which significantly diminish the efficiency and performance of fuel cells. Consequently, research interests have also gradually been extended to the development of non-Pt electrocatalysts, such as other noble metals,[14-16] non-noble metals,[17-20] and metal-free materials.[21]

Among these alternates, palladium (Pd)-based electrocatalysts have received broad attention due to their similar electronic structures, comparable performance, and perhaps lower cost than Pt. Recent progress of the extensive investigations has also demonstrated that the pure Pd and Pd-based electrocatalysts exhibit superior catalytic activity and stability in alkaline media in comparison with Pt.[14-16, 22-26] In addition, it was determined that Pd-based electrocatalysts exhibited much higher methanol tolerance and resistance to CO as compared with Pt-based electrocatalysts. As such, developing cost-effective and high-efficient Pd-based electrocatalysts for substantially enhancing ORR performance is highly desirable and essential, especially in alkaline media.[27] However, they still cannot attain all the requirements for the implementation of fuel cells, where ORR electrocatalysts are expected to possess the features of low cost, high activity, and high stability synchronously. To this end, various strategies have been developed for further improving the electrocatalytic performance of Pd-based electrocatalysts with precise control over the shape, composition, crystal phase, and surface strain while observably decreasing the Pd usage, since these structural parameters play crucial roles in determining their ORR performance.[28-32] For example, well-defined PdCu nanocubes enclosed by {100} facets exhibited enhanced ORR performance in 0.1 M KOH as compared with polycrystalline-exposed PdCu nanoparticles and Pd nanoparticles, confirming that the ORR performance can be boosted by both the shape and composition optimization.[33] DiSalvo and coworkers also demonstrated that ordered intermetallic Pd_3Pb nanocrystals exhibited excellent electrocatalytic activity toward ORR in alkaline media as compared with their counterparts in a disordered phase.[34] Moreover, as validated by a recent report, the tensile-strained surface of PdFe alloy enabled the optimum binding strength for reaction intermediates, ultimately resulting in the maximum activity toward ORR in 0.1 M KOH.[35] Concisely, increasing attention has been turned to the rational design of novel approaches to elaborately modulate the nanoscale features of Pd-based electrocatalysts.

Although several reviews concentrating on Pd-based electrocatalysts have been released in the past years,[36-41] a comprehensive and systematic summary on delicately designing the nanoscale structures of Pd-based electrocatalysts using various strategies, especially with high-efficient ORR in alkaline media, is still very intriguing. In this review, we focus on addressing the fundamental ORR mechanisms of Pd-based electrocatalysts in alkaline media and the most commonly used strategies for achieving their structures with tunable ORR performance. Furthermore, we highlight some of the current challenges and future perspective directions related to the controllable synthesis of Pd-based electrocatalysts with substantially improved ORR performance in alkaline media. To the best of our knowledge, by far there has been no report that attempts to cover these advances of Pd-based ORR electrocatalysts in alkaline media.

2. Fundamental ORR Mechanisms of Pd-based Electrocatalysts in Alkaline Media

Given its significant prominence in fuel cell devices, the ORR has recently received increasing attention, especially in alkaline media, due to the greatly enhanced kinetics as compared with the acidic media.[27, 42, 43] Presently, the Pd-based electrocatalysts are generally considered to be one of the most promising candidates for replacing Pt while maintaining the high catalytic performance for ORR in alkaline media.[25, 38] It has also been identified that the ORR efficiency on Pd-based electrocatalysts in alkaline media can be comparable or superior to that of Pt/C, mainly owing to the declining influence from adsorption of anions.[42] Typically, the ORR process requires the cleavage of strong O-O bonds and involves the multiple electron transfer steps, which often leads to undesirable side reactions and a high overpotential, ultimately degrading the electrocatalytic performance in the devices.[44-46] As such, it is highly desirable to understand the ORR mechanism in atomic-scale in order to develop high-efficient ORR electrocatalysts.

Compared to Pt-based electrocatalysts, the insightful ORR mechanisms on the surface of Pd-based electrocatalysts in alkaline media have not been completely understood despite the extensive efforts over the past decades.[47-49] Nonetheless, the ORR process on Pd-based electrocatalysts should be akin to that on Pt-based analogs due to their similar surface features.[38] It is generally recognized that the complete ORR process involves four coupled proton and electron transfers, which may couple with several possible pathways in alkaline media:

(1) O_2 reduction to OH^- ions via a direct four-electron pathway,

(2) O_2 reduction to H_2O_2 via a two-electron pathway,

(3) a combination of four and two-electron pathways,

(4) an associative mechanism involving the adsorption of O_2 and direct proton/electron transfer to O_2 and OOH, which contributes to the formation of O and OH,

(5) a dissociative mechanism involving the cleavage of O-O bonds of O_2 and the hydrogenation of O to OH.

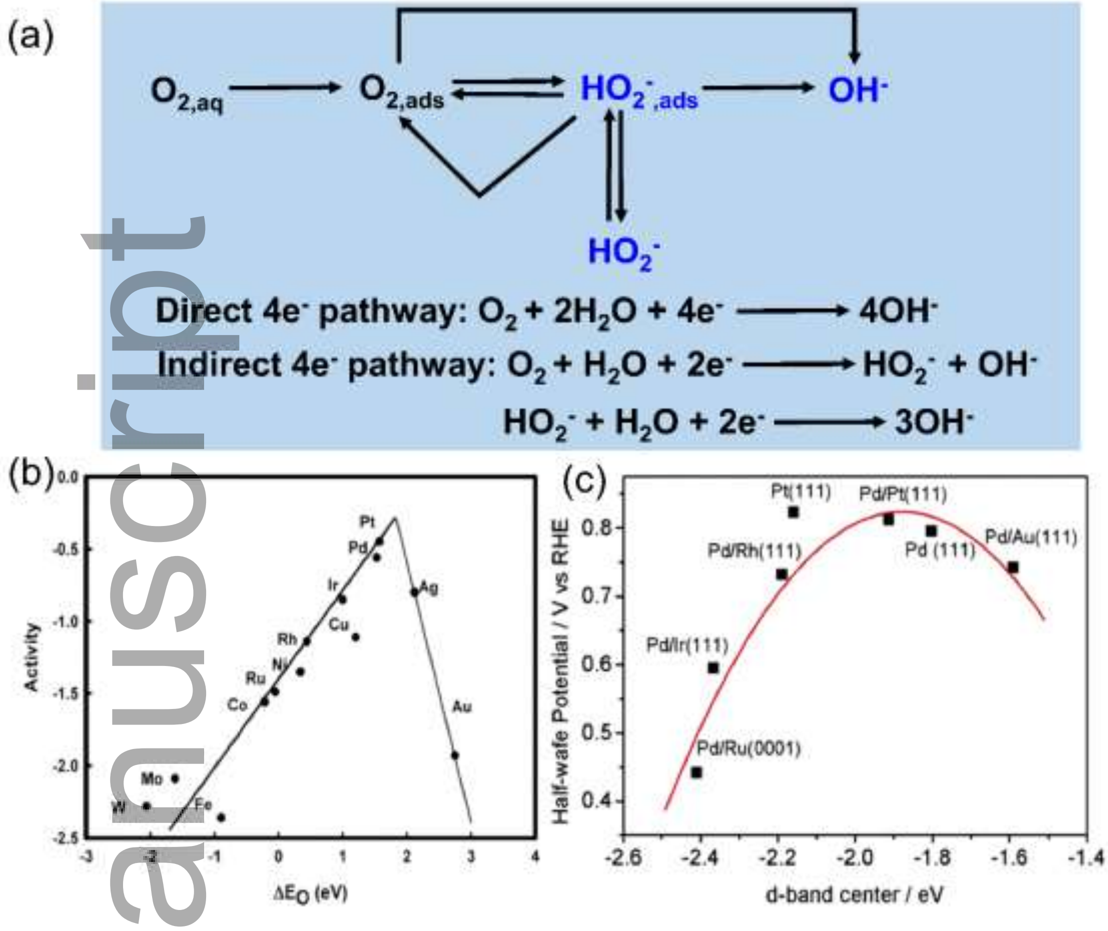

Figure 1. a) Schematic illustration of alkaline ORR mechanisms and the possible intermediates on the surface of Pd-based electrocatalysts. b) Variation trends in ORR activity of different electrocatalysts plotted as a function of the oxygen-binding energy. Reproduced with permission.[50] Copyright 2004, American Chemical Society. c) Volcano plot of the half-wave potential of Pd-based electrocatalysts *vs.* the calculated Pd *d*-band center relative to Fermi level. Reproduced with permission.[51] Copyright 2006, American Chemical Society.

Specifically, according to the general ORR mechanism proposed by Anastasijevic and coworkers[52] shown in Figure 1a, an ORR process typically undergoes the following major steps:

$$O_{2,\,ads} + e^- \rightarrow O_2^- \quad (1)$$

$$O_2^- + H_2O + e^- \rightarrow HO_2^- + OH^- \quad (2)$$

$$HO_2^- + e^- \rightarrow O^- + OH^- \quad (3)$$

$$O^- + H_2O + e^- \rightarrow 2OH^- \quad (4)$$

$$O_{2,\,ads} \rightarrow 2O_{ads} \quad (5)$$

$$O_{ads} + e^- \rightarrow O^- \quad (6)$$

$$O^- + H_2O + e^- \rightarrow 2OH^- \quad (7)$$

For the 4e$^-$ pathway, it articulates that the molecular oxygen adsorbed on the catalyst surface would generate O_2^- intermediate when catching an electron in the first step. The O_2^- intermediate then further incorporates with an electron and water, facilitating the formation of species HO_2^- and OH^-. Finally, the HO_2^- is further reduced to OH^- once receiving an additional electron. In contrast, another possible pathway involves a formation of absorbed O species from the dissociation of O_2 and a subsequent reduction to O^- and then to OH^-. Note that it was typically recognized that the rate-controlling step of ORR is the first electron-transfer reaction or O_2 adsorption along with the superoxide anion production in alkaline media.[53] Based on the previous reports,[5, 27] it seems that the 4e$^-$ pathway, without hydrogen peroxide (H_2O_2) intermediates, is more favorable on Pd-based electrocatalysts. The H_2O_2 intermediates, yielding in the 2e$^-$ pathway, are typically harmful species and could not only corrode the electrocatalysts but also markedly decrease energy conversion efficacy in the fuel cell devices. It should be emphasized that the presence of Pd-oxides on the catalyst surface might promote the formation of H_2O_2 via the 2e$^-$ pathway.[54] Meanwhile, the alkaline ORR mechanism on Pd-based electrocatalysts is highly dependent on the potential range applied, which can be utilized to effectively regulate the exposure of Pd active sites.[55] Furthermore, to further interpret the ORR activity on different electrocatalysts, Nørskov and coworkers established a linear correlation associated with the oxygen–metal bond interactions and the position of metal *d* states relative to Fermi level based on the density functional theory (DFT) calculations (Figure 1b), which called a *d*-band center theory.[50] Specifically, the apparent discrepancy of the oxygen–metal bond mainly depends on the coupling strength between the O 2*p* states and the metal *d* states.[56] In theory, an upward shift of the *d* states will cause an upward shift of the anti-bonding states, resulting in a stronger bond and thus unfavorably removing O and OH species adsorbed on the surface. Therefore, a close relationship between the electronic structure of the metallic catalyst and catalytic activity can be well-established, which provides an effective approach to search for high-efficient catalysts for the ORR. More importantly, by further calculating the adsorption energy of the surface intermediates during the ORR process as demonstrated by Adzic and coworkers, a nice volcano plot shown in Figure 1c can be obtained, where Pd-based electrocatalysts possess the moderate oxygen-binding energy, not too high or too low, which is very suitable as the ORR electrocatalysts.[51] Based on these previous findings, it is reasonably envisioned that there is still plenty of room for ORR performance improvement by elaborately designing the electrocatalyst structure, such as alloying, optimizing the surface metal and/or structure, and tuning the phase structure.

For the convenience of the following discussion, the reported ORR activities of some pure Pd nanoparticles supported on carbon (Pd/C) in alkaline media are summarized in Table 1.

Table 1. Summary of the ORR activities of some Pd/C electrocatalysts reported previously

Catalyst details	Mass activity (A/mg_{Pd}^{-1})	Specific Activity (mA/cm_{Pd}^{-2})	Measured potential and reference electrode	Electrolyte	Reference
Commercial 10 wt% Pd/C	0.18	0.52	0.9 V *vs.* RHE	0.1 M KOH	[57]
Commercial 20 wt% Pd/C	0.02	0.038	0.9 V *vs.* RHE	0.1 M KOH	[58]
	0.035		0.875 V *vs.* RHE	0.1 M KOH	[58]
Synthesized 10 wt% Pd/C	0.07	0.03	0.91 V *vs.* RHE	0.1 M KOH	[59, 60]
Synthesized 20 wt% Pd/C	0.28	0.55	0.85 V *vs.* RHE	0.1 M NaOH	[61]
	0.75		0.80 V *vs.* RHE	0.1 M NaOH	[61]
Synthesized 20 wt% Pd/C		0.19	0.9 V *vs.* RHE	0.1 M KOH	[62, 63]
Synthesized Pd/C	0.11	0.07	0.86 V *vs.* RHE	0.1 M KOH	[64]
	0.04	0.01	0.91 V *vs.* RHE	0.1 M KOH	[64]
Synthesized Pd/C	0.34		- 0.1 V *vs.* Hg/HgO	0.1 M KOH	[65]

3. Strategies to Enhance Alkaline ORR Performance of Pd-based Electrocatalysts

To acquire the highly efficient Pd-based ORR electrocatalysts, it is very essential to master the commonly used strategies to rationally design the electrocatalysts structures at the atomic scale. In this part, we outline several strategies of the structure design for improving the alkaline ORR performance of Pd-based electrocatalysts, including shape and size control, phase control, heteroatom doping, surface-strain control, and de-alloying, and elaborate on their recent progress.

3.1 Shape and Size Control

Extensive efforts have been devoted to the manipulation of shape- and size-controlled Pd-based electrocatalysts for improving their electrochemical performance in the past two decades.[33, 66-71] It is generally believed that exposure on a particular catalyst surface and specific size may favor an electrocatalytic reaction, and this could provide a better understanding of the shape- and size-dependent performance.[13, 72-74] To this end, various approaches have been widely developed to precisely tune the morphology of Pd-based electrocatalysts for their catalytic performance enhancement.[75-77] Of central importance for the shape-control is the elaborate choice of experimental parameters, such as appropriate reducing agents, solvents, coordination ligands, capping agents, surfactants, and foreign ions as the chemical additives, that are capable of selectively binding to specific facets on the nanocrystal and markedly altering the growth rates of different facets.[69] For size control, the use of these chemical additives in a synthetic system could typically modulate the nucleation and growth kinetics through coordination. It should be pointed out that these chemicals could strongly bind to surfaces of the yielded nanocrystals, seriously impeding their subsequent practical application. To avoid the negative influence, however, complete removal of species adsorbed on the particle surfaces is generally required and should be carefully considered before the performance tests. As demonstrated by Guo and coworkers, PdMo bimetallene in highly curved and sub-nanometre-thick metal nanosheet was achieved by simultaneously reducing $Pd(acac)_2$ and $Mo(CO)_6$ by ascorbic acid in the presence of oleylamine.[78] The key to the successful synthesis is highly dependent on the decomposition temperature of the metal carbonyl precursors and the type of reducing agents. Interestingly, they reported that the as-synthesized PdMo bimetallene showed an electrochemically active surface area as large as 138.7 $m^2\ g_{Pd}^{-1}$, resulting in a mass activity up to 16.37 A mg_{Pd}^{-1} toward ORR at 0.9 V in alkaline media, which is 78 times and 327 times as high as those of Pt/C and Pd/C commercial catalysts, respectively. They ultimately concluded that the synergistic effect, the strain effect induced by the curved morphology, and the quantum-size-effect derived from supra-thin nanosheets could dramatically alter the electronic structure with optimal oxygen-binding based on the DFT calculations. Later, Huang and coworkers developed a template-directed approach for the synthesis of ultrathin PdM (M = Pb, Sn, and Cd) porous nanosheets with desirable sizes (Figure 2a).[79] In this case, the use of Pd ultrathin nanosheets as the template (Figure 2b) plays an important role in directing the morphological development and regulating the deposition of foreign atoms as well as the subsequent interatomic diffusion. As expected, the ORR mass activity of the ultrathin Pd_3Pb porous nanosheets is 6.8 times as high as that of the Pt/C in 0.1 M KOH solution, with remarkable stability (Figure 2c). The DFT calculations also suggested that the interatomic interaction between Pd and Pb could optimize the surface electronic structure, thus boosting the ORR performance. This work showcases an improved ORR performance through delicate controlling the morphology of Pd-based electrocatalysts in nanosheets as the ultrathin-sheet could provide abundant active sites, high conductivity, and high atomic utilization.[37]

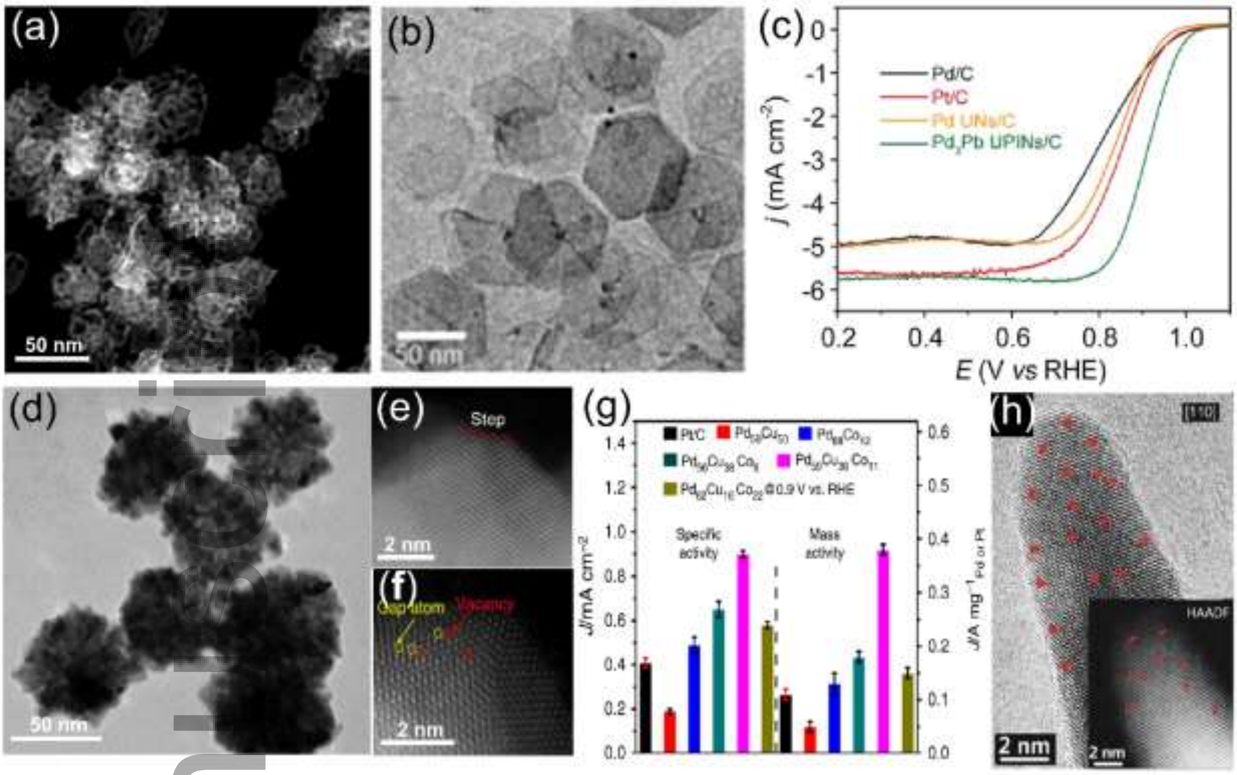

Figure 2. a) HAADF-STEM image of Pd_3Pb ultrathin porous intermetallic nanosheets. b) TEM image of Pd ultrathin nanosheets. c) ORR polarization curves recorded in O_2-saturated 0.1 M KOH electrolyte at a scan rate of 10 mV s^{-1} and a rotation rate of 1600 rpm. a-c) Reproduced with permission.[79] Copyright 2021, Wiley-VCH. d) TEM image of the as-synthesized dendritic $Pd_{59}Cu_{30}Co_{11}$ nanoalloys. e, f) Defect analysis images of the as-synthesized dendritic $Pd_{59}Cu_{30}Co_{11}$ nanoalloys through aberration-corrected TEM. g) Specific activities and mass activities of the Pt/C, $Pd_{88}Co_{12}$, $Pd_{50}Cu_{50}$, $Pd_{56}Cu_{38}Co_6$, $Pd_{59}Cu_{30}Co_{11}$, and $Pd_{62}Cu_{16}Co_{22}$ catalysts toward ORR at 0.9 V. d-g) Reproduced with permission.[80] Copyright 2018, Springer Nature. h) HRTEM image of a dendritic structure projected along the zone axes of [110] axis. The inset in (h) is the corresponding HAADF-STEM image. Reproduced with permission.[81] Copyright 2018, Wiley-VCH.

Unlike the 2D nanosheet, the anisotropic dendritic morphology of Pd-based electrocatalysts has also been proved to be high-efficient for substantially improving the ORR performance owing to the large specific surface area, high densities of stepped atoms, and abundant defect sites that presented on the corners and edges.[80, 82, 83] In a recent report, Wang and coworkers reported their synthesis of dendritic PdCuCo nanoalloys, serving as robust multifunctional electrocatalysts for ORR in 0.1 M KOH (Figure 2d).[80] Particularly, the composition of the as-synthesized nanoalloys could be readily tuned by merely varying the feeding molar ratios among the precursors, while the dendritic morphology was preserved. Impressively, the $Pd_{59}Cu_{30}Co_{11}$ nanoalloys exhibit superior activity and durability toward ORR compared with the Pt/C catalyst, mainly due to the presence of abundant defects for this special dendritic nanostructure (Figure 2e-g). In another example, Han and coworkers disseminated a general synthesis approach for a class of multicomponent anisotropic dendrites with abundant vacancies.[81] The presence of atomic vacancies from the ternary PdCuCo dendrites was shown clearly (Figure 2h) based on the high-resolution transmission electron microscopy characterization. Benefiting from the vacancies sites on the surface, the optimized electronic structures of these PdCuCo nano-dendrites can significantly accelerate the charge transfer in the ORR process, thereby exhibiting substantial enhancement in mass activity and stability. Consequently, modifying the electronic structure of the Pd-based electrocatalysts via a generation of the dendritic morphology with rich defects/vacancies is an intrinsic regulatory strategy to boost its ORR performance in alkaline media. Furthermore, this morphology-based strategy has also been widely demonstrated using other shapes of Pd-based electrocatalysts, such as nanocubes, nanorods, and nanoplates, which showed excellent activity and stability toward ORR in alkaline media.[33, 84-87]

Except for the shape-control strategy mentioned above, size control was also proved to be effective for improving the ORR activity of Pd-based electrocatalysts.[88, 89] Since heterogeneous catalysis occurs on the surface of catalysts, maximum exposure of catalyst surface atoms is desired. The fraction of catalyst surface area can be readily tuned by merely controlling the catalyst size. As such, single-atom catalysts (SACs) would be an extreme case.[90-94] In fact, the delicate design and development of SACs are recently emerging as a new frontier in the electrocatalysis field.[95, 96] It has been reported that Pd-based SACs exhibit great potential in enabling maximum atom-utilization with unique geometric and electronic properties that are derived from the lack of metal–metal bonds and the ionic nature of the isolated catalytic sites.[97, 98] For example, Sun and coworkers developed a one-pot hydrothermal approach to prepare atomically dispersed Pd catalysts supported on carbon nanotubes and manganese oxide nanowire networks and showed a superior Pd mass activity (484 A g^{-1} at 0.9 V) for ORR in alkaline media when compared to state-of-the-art Pd-based electrocatalysts.[99] Experimental and theoretical studies affirmed that Pd single atoms and the surrounding metal sites synergistically contributed to activating molecular oxygen and optimizing the binding strength to reaction intermediates. This could significantly accelerate the ORR kinetics.

3.2 Phase Control

For Pd-based electrocatalysts, optimizing their catalytic performance by tuning the phase has become a novel and versatile strategy.[29, 100-102] Some unconventional phases that are difficult to attain in their bulk state could be stable in their nanostructure and endow these Pd-based electrocatalysts with intriguing properties, paving the way for understanding the phase-dependent performance.[103] As discussed in recent years, relative to a random alloy, the ordered intermetallic structures with a specific atom stoichiometry and a long-range atomic ordering present remarkable properties toward a broad range of applications, especially electrocatalysis, owing to the enhanced interaction between different components.[104-106] It is worth noting that the synthesis of Pd-based nanocrystals with an unconventional phase structure is often highly challenging due to the competitive formation of the thermodynamically stable phase. Accordingly, some effective strategies might need to be further developed to stabilize the unconventional phases and maintain their excellent electrocatalytic performance, since the unconventional phases are generally recognized to be thermodynamically unstable. Goodenough and coworkers demonstrated that an ordered Pd_3Fe/C intermetallic electrocatalyst prepared through a thermal annealing approach with the aid of a KCl matrix showed significantly enhanced activity and durability for ORR under alkaline conditions, as compared with the disordered Pd_3Fe/C, Pd/C, and Pt/C catalysts.[107] They claimed that such an enhancement originated from remarkable changes in the Pd−Pd bond distance and electron structure as well as the presence of uniform active sites. Huang and coworkers further developed a new strategy for the synthesis of $L1_2$-ordered Pd_3Pb tripods with predominant {110} facets by co-reducing $Pd(acac)_2$ and $Pb(acac)_2$ in a mixed solvent of oleylamine and oleic acid (Figure 3a).[108] Based on the first-principle calculations, they believed that the strongly coupled *s-p-d* exchange effect on {110}faceted Pd_3Pb tripods with ordered structure played a crucial role in greatly boosting the ORR performance (Figure 3b). As such, the controlled synthesis of Pd-based electrocatalysts with ordered intermetallic structures offers an alternative avenue to substantially promoting their ORR performance.

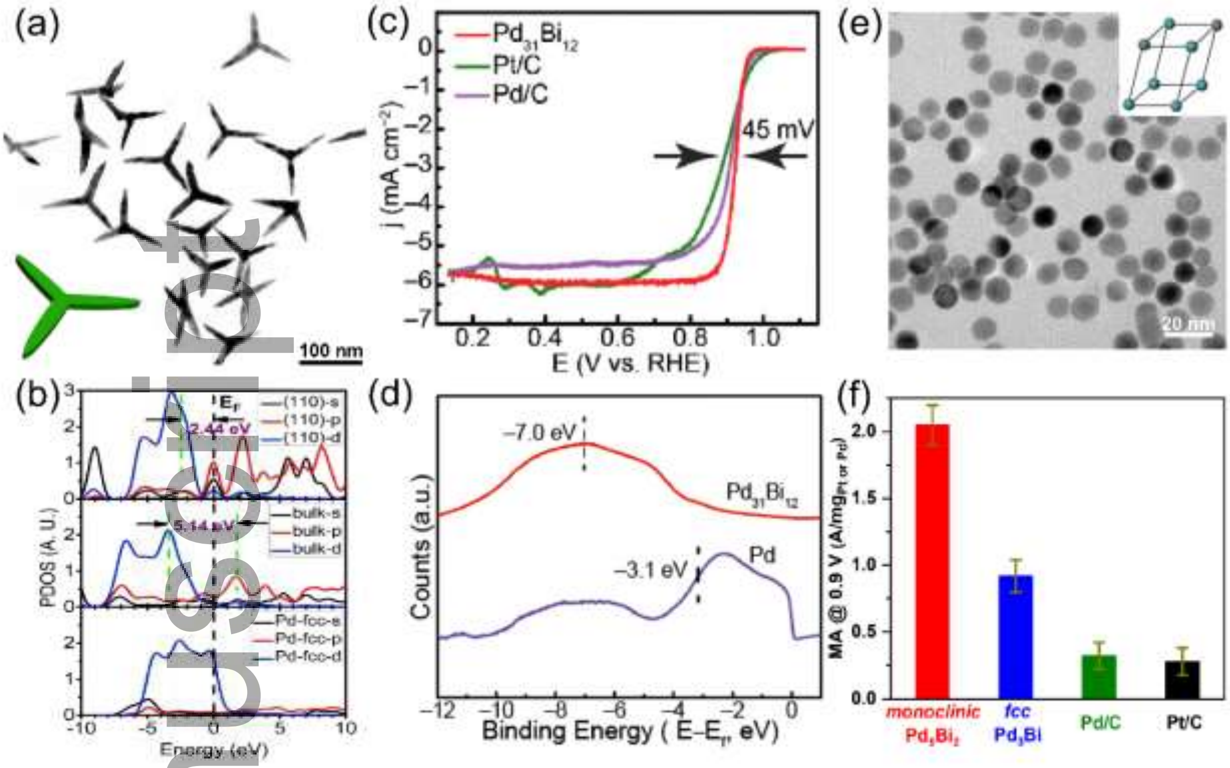

Figure 3. a) TEM image of $L1_2$-ordered Pd_3Pb tripods with the corresponding structural model as the inset. b) Combined projected DOS of metallic Pd, bulk Pd_3Pb, and $L1_2$-ordered Pd_3Pb (110) surface. a-b) Reproduced with permission.[108] Copyright 2018, Cell Press. c) ORR polarization curves of $Pd_{31}B_{12}$, Pd/C, and commercial Pt/C catalysts measured in O_2-saturated 0.1 M KOH solution at a rotational speed of 1600 rpm. d) Valence band spectra of $Pd_{31}Bi_{12}$ and Pd foil measured by ultraviolet photoelectron spectroscopy (UPS) with a He I source. c-d) Reproduced with permission.[109] Copyright 2019, American Chemical Society. e) TEM image of monoclinic Pd_5Bi_2 nanocrystals with the corresponding structural model as the inset. f) Mass activities of the monoclinic Pd_5Bi_2/C, face-centered cubic (*fcc*) Pd_3Bi/C, Pd/C, and Pt/C at 0.9 V *vs.* RHE. Reproduced with permission.[29] Copyright 2021, American Chemical Society.

In addition, it has recently been reported that some unconventional phases of Pd-based electrocatalysts, such as rhombohedral, monoclinic, and orthorhombic phases, exhibit remarkable activity and stability toward ORR in alkaline media.[29, 102, 109] For example, Hall and coworkers utilized the electrodeposition approach to prepare metastable $Pd_{31}Bi_{12}$ nanocrystals with a rhombohedral crystal structure at room temperature in minutes.[109] It was identified that the $Pd_{31}Bi_{12}$ nanocrystals are highly efficient for ORR, yielding specific activities over 35 folds as high as those of the Pt/C and Pd/C catalysts (Figure 3c). Valence band spectra of the $Pd_{31}Bi_{12}$ verified that the adsorption energy of ORR intermediates for $Pd_{31}Bi_{12}$ is reduced with a shift to the optimal value, which could be a major reason for the ORR improvement (Figure 3d). Most recently, we reported uniform Pd_5Bi_2 nanocrystals with a monoclinic structure synthesized using a facile one-pot approach. These monoclinic Pd_5Bi_2/C nanocatalysts exhibit a mass activity up to 2.05 A/mg$_{Pd}$ toward

ORR in 0.1 M KOH (Figure 3e and 3f).[29] Owing to the enhanced electron interaction between Pd and Bi components in Pd_5Bi_2, the leaching of the Bi could also be greatly alleviated during the ORR process, resulting in extraordinary stability. While various unconventional phases are being continuously developed for improving catalytic performance, it is foreseeable that this concept could also be extended to other Pd-based multimetallic systems successfully.[110-114]

3.3 Heteroatom Doping

Heteroatom doping has recently emerged as an effective method for developing highly stable and active Pd-based electrocatalysts.[115-119] It has been unveiled to be highly effective for regulating the electronic structure, boosting the reaction kinetics, optimizing the binding affinity with reaction intermediates, and modifying the surface characteristics.[120] It is often required to purposely take into account the discrepancies in the mutual solubility and electronegativity between the host matrix and the dopants. The dopants can be generally classified into metal and nonmetal atoms. Metal doping is also called alloying, and it can introduce more active sites, optimize electronic structures, and greatly improve the performance of a catalyst derived from the synergistic effect of different metal components during the practical ORR process. In contrast, it was found that nonmetal doping can polarize the surrounding atoms due to the high electronegativity of nonmetals, significantly vary the band centers of the active sites and thus enhance electrocatalytic performance. Inspired by these findings, extensive efforts have been made on the delicate design of high-performance Pd-based electrocatalysts by heteroatom doping in recent years.[48, 121-124] By doping various metals, such as copper (Cu), bismuth (Bi), Pt, silver (Ag), gold (Au), cobalt (Co), nickel (Ni), and so on, the ORR activity and stability of Pd could be dramatically enhanced in alkaline media.[23, 29, 125-129] For example, Abruña and coworkers recently prepared a series of Pd−Cu thin-film with tunable composition using a magnetron sputtering approach and then evaluated their ORR performance in 1 M KOH (Figure 4a and 4b).[130] Among the samples, $Pd_{50}Cu_{50}$ binary alloy was identified as the most promising electrocatalyst toward ORR, showing a remarkable mass activity (more than 3-fold greater than that of Pd/C catalyst, Figure 4c). This activity enhancement may be attributed to an optimal *d*-band center derived from electron redistribution of Pd and Cu atoms. Previously, Henkelman and coworkers studied composition-dependent ORR performance on PdCu nanoparticles based on DFT calculations.[131] They probed that charge transfer from Cu to Pd would contribute to up-shifting the *d*-band center of Cu and down-shifting that of Pd, giving rise to stronger binding between O and Cu and weaker binding between O and Pd. It was also reported that ternary PdCuNi and PdCuCo electrocatalysts with an ordered structure possess higher activity and stability toward ORR as compared with the binary PdCu and the Pd/C catalyst.[103] An introduction of smaller-sized atoms, Co and Ni, into the PdCu lattice could facilitate the formation of catalytically active and hollow sites on the surface together with the optimal electronic structure, which improved ORR activity and stability. All together, the electronic structure and Pd density of states could be dramatically altered by doping foreign metallic atoms, which provides a universal strategy for boosting the electrocatalytic performance.

Pd catalysts could also be modified using nonmetal atoms, such as hydrogen (H) and boron (B), to optimize their electronic structure as a promising strategy demonstrated in recent years.[132-134] It should be pointed out that nonmetal elements with small atomic radii and favorable affinity are typically capable of permeating into interstitial sites within the Pd lattice, which could profoundly turn the lattice parameters and charge transfer energy between different components. For example, H could easily implant in the Pd lattice to form Pd hydrides as the key intermediates especially during the electrocatalytic process.[135] Huang and coworkers developed a wet-chemical approach for successfully preparing H-implanted Pd icosahedra with enhanced ORR activity and stability.[136] It was verified that the H-implanted Pd icosahedra could greatly decrease electronic densities and weaken the Pd–O binding strength, thus significantly boosting the electrocatalytic performance as compared with the structure without H doping. In this case, the twinned {111} facets in H-implanted Pd icosahedra are also vital to effectively decrease the ORR barrier and stabilize the intermediated species. Moreover, the ORR performance is highly dependent on the hydride degree in the Pd nanocrystals, as confirmed by Wang and coworkers.[137] Such an approach of interstitial H atom doping can also be extended to other Pd-based nanostructures with enhanced catalytic performance.[138, 139]

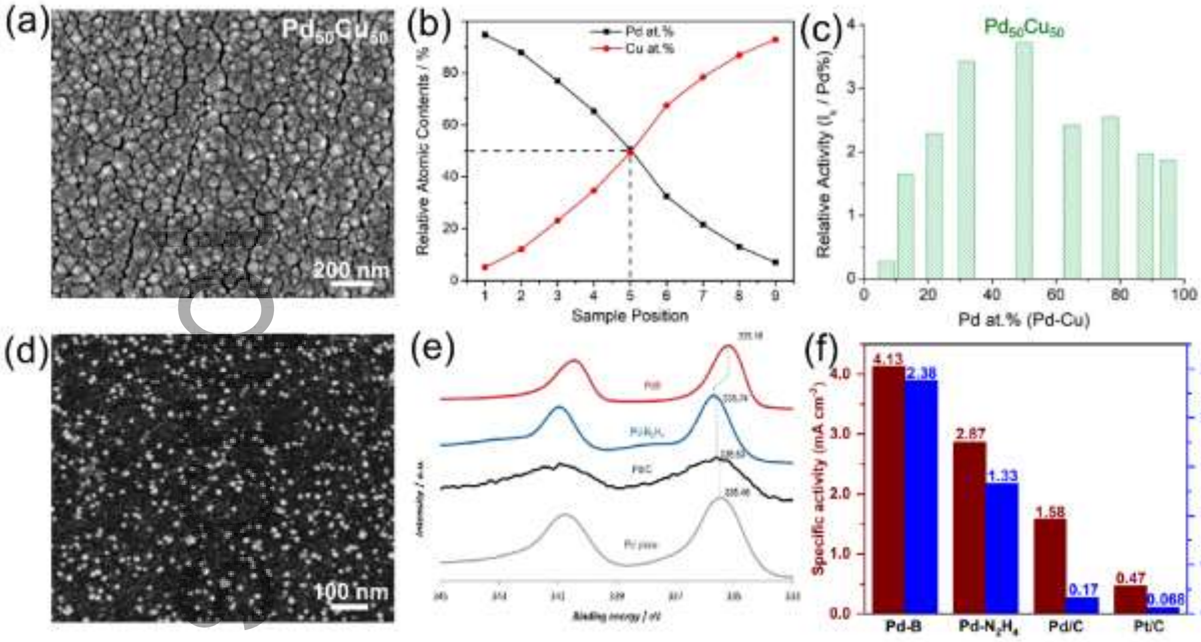

Figure 4. a) SEM image of $Pd_{50}Cu_{50}$ with an average size of around 100 nm. b) Relative atomic contents of Cu and Pd as a function of the sample position, which covers the range of Cu at. % from ~5% to ~95% with $Pd_{50}Cu_{50}$ in the middle. c) Relative ORR activity calculated by normalizing the kinetic current to the Pd at. % *vs.* Pd at. % in the samples. a-c) Reproduced with permission[130] and modified. Copyright 2020, American Chemical Society. d) SEM image of Pd–B nanoparticles. e) XPS spectra of Pd–B, Pd–N_2H_4, commercial Pd/C, and Pd plate. f) Comparisons in specific activities and mass activities of Pd–B, Pd–N_2H_4, and commercial Pd/C catalysts in O_2-saturated 0.1 M KOH solution, based on the data reported in ref.[140] d-e) Reproduced with permission.[140] Copyright 2016, Wiley-VCH.

Besides, doping B into Pd-based electrocatalysts equally becomes a universal approach to deliberately regulate the electronic structure and enhance their electrocatalytic performance.[141, 142] It should be emphasized that doping B could generally cause the downshift of the *d*-band center derived from the electron transfer between the *d*-orbitals of Pd and *p*-orbitals of B. As demonstrated by Sato and coworkers, B-doped Pd could decrease the barrier of O_2 dissociation and optimize the binding energy of ORR intermediates, recognizing that Pd-B is highly active for ORR in alkaline media (Figure 4d).[140] Relative to undoped Pd catalyst, Pd-B synthesized by an electroless deposition approach yields a mass activity of 2.38 A/mg$_{Pd}$ at 0.90 V, achieving a 14-fold enhancement. X-ray photoelectron spectra and computational results indicate a negative shift of the Pd binding energy after a B-doping and suggest that such doping fills the density of states with excessive electrons, significantly weakening the O-bonding to Pd and enhancing the ORR performance (Figure 4e and 4f). By employing a different approach, Chen and coworkers carried out a one-pot synthesis of Pd-B nanocrystals in N, N-dimethylformamide using $NaBH_4$ as a reductant and dopant.[143]

They reported that Pd-B nanocrystals with different boron contents could be readily obtained by precisely controlling the reaction time and concentration of $NaBH_4$. The as-synthesized Pd-B ORR nanocatalysts show a mass activity is 14 times as high as that of the commercial Pt/C catalyst in alkaline solution (Figure 4f). The improvement in ORR performance was found to associate with the presence of sub-oxidized B on the outermost surface and B in the subsurface. In both cases, the presence of B in Pd-based electrocatalysts gave rise to highly enhanced ORR performance in alkaline media.

Furthermore, it seems that doping Pd-based electrocatalysts with different nonmetal elements is also a feasible strategy to tune their surface electronic structures and boost their ORR performance.[144, 145] Liu and coworkers developed a soft-templating approach to co-alloyed Pd with B and phosphorus (P) to construct Pd-B-P ternary mesoporous nanospheres using dimethylamine borane and sodium hypophosphite as the sources of B and P, respectively.[146] Benefiting from the three-dimensional dendritic morphology with highly exposed active sites and the B/P co-doping with optimized surface electronic structure, this ternary system exhibits excellent ORR activity and stability as compared with the undoped and single-element doped counterparts. This approach was further extended to a multi-component PdM´BP nanosphere system (M´ = Cu, Ag, and Pt) nanospheres, showing expected achievement.[50] In a remark, rationally altering the electronic structure of a Pd-based catalyst by doping with heteroatoms could be another viable strategy for substantially promoting their ORR performance.

3.4 Surface-Strain Control

Surface strain can be caused by either tensile or compressive force and quantified as the alteration in bond length for surface atoms as compared with the ideal bulk value. Generally, a distortion of a crystal lattice away from the ideal value is often caused by tension at the interface between two different phases, including twinned boundary, facet, and core-shell structure. It is important to note that this kind of strain effect will approach the strongest on the interface and then rapidly decrease with the increase of distance from the surface. Particularly, the expansion and contraction of bonds diminish and enlarge the overlap between *d*-electron orbitals of the affected atoms, respectively, ultimately inducing the changes of the *d*-band center and thus affecting the binding strength of absorbed species on the catalyst surface. Consequently, the surface strain provides an alternative strategy to maximize the electrocatalytic performance in a reaction.[147-

[152] It should be emphasized that insightful efforts might need to be further made to accurately induce and modulate the surface strain to the desired level on the surface of nanocatalysts without compromising other structural parameters. In some cases, atom diffusion, defect formation, and surface reconstruction may lead to releasing the surface strain during the practical electrocatalytic process. For instance, Sun and coworkers synthesized a series of uniform core–shell nanocrystals composed of an Au (or Ag) core and PdCu-alloy shell and demonstrated excellent catalytic activity and stability toward ORR in alkaline media.[153] By merely regulating the molar ratio of $Pd(acac)_2$ to $Cu(acac)_2$, the thickness and composition of the PdCu shell could be precisely tuned in this work. In 0.1 M KOH, both $Ag@Cu_{37}Pd_{63}$ and $Au@Cu_{40}Pd_{60}$ samples (with shell-thickness of 0.75 and 1.1 nm, respectively) delivered mass activity of ~0.20 A/mg (noble metal basis), which is over 3 times as high as that from the commercial Pt/C (0.06 A/mg_{Pt}). Supported by DFT calculations, they further ascribed the electrocatalytic activity enhancement to the optimized surface strain and electronic structure on the shell by comparing another group of core–shell catalysts M″@CuPd (M″ = Au and Ag) with different Cu/Pd molar ratios as well as the CuPd nanoparticles and Pd/C catalyst (Figure 5a-c). Subsequently, Zhuang and coworkers reported a spontaneously galvanic displacement approach to successfully prepare a Pd skin onto the AuCu ordered intermetallic nanoparticles (Figure 5d).[154] It has been confirmed that the AuCu ordered intermetallic core was fully coated with a Pd shell with 2–3 atomic layers, and also verified that the AuCu@Pd core-shell nanoparticles exhibit extraordinary stability in alkaline solution and their ORR mass activity is ~20 times as high as that of the commercial Pt/C catalysts (Figure 5e). Similarly, this outstanding performance was attributed to the lattice shrinkage in Pd induced by the AuCu ordered intermetallic core and thus the significant weakening of the oxygen affinity on the Pd shell. As demonstrated by a theoretical study,[155] the surface strain effect on the strength of Pd–O binding was also found to be highly shape-dependent on Pd-based core-shell electrocatalysts. Based on the first-principles and multiscale quantum mechanics/molecular mechanics, Lu and coworkers revealed linear scaling relationships between the oxygen adsorption energy and surface strain, which can be determined from nanocrystal facets and edges (Figure 6). By systematically evaluating the ORR activity on Pd-based core-shell nanoparticles as a function of their shapes, it was suggested that the compressive strain on the {111} facets and the edges favor the ORR, whereas the compressive strain on the {100} facets suppresses the ORR. Taken together, constructing a Pd-based core-shell electrocatalyst with tunable compressive strain could efficiently enhance their ORR performance in alkaline media while the cost is significantly reduced.

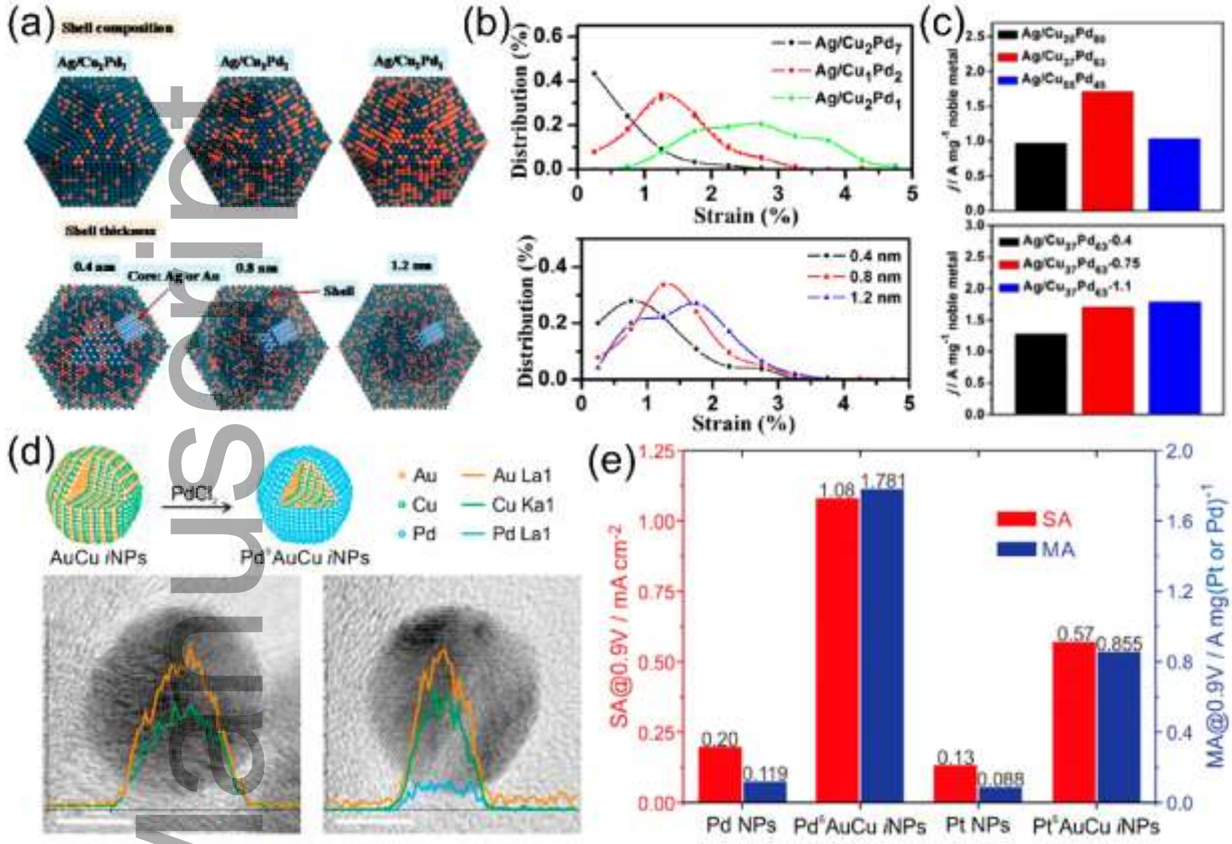

Figure 5. a) Models of core-shell nanoparticles for different shell compositions with a shell thickness of 0.8 nm and core-shell nanoparticles for different shell thickness with a shell composition of $CuPd_2$. b) Calculated distribution of surface strain on core-shell nanoparticles with different shell compositions with a shell thickness of 0.8 nm and core-shell nanoparticles for different shell thickness with a shell composition of $CuPd_2$. c) Comparisons in mass activity at −0.2 V of Ag@CuPd nanoparticles with different shell composition and thickness in O_2-saturated 0.1 M KOH solution at a scan rate of 10 mV/s and a rotation rate of 1600 rpm. a-c) Reproduced with permission.[153] Copyright 2014, American Chemical Society. d) Schematic illustration of the synthesis of Pd skin on ordered intermetallic AuCu nanoparticles through the galvanic replacement approach, and TEM images of an ordered intermetallic AuCu nanoparticle and AuCu@Pd core-shell nanoparticle, together with the corresponding STEM-EDX line scans along a single nanoparticle. e) Comparisons in specific activity and mass activity in O_2-saturated 1.0 M KOH at 0.9 V *vs.* RHE. d-e) Reproduced with permission[154] and modified. Copyright 2016, Elsevier.

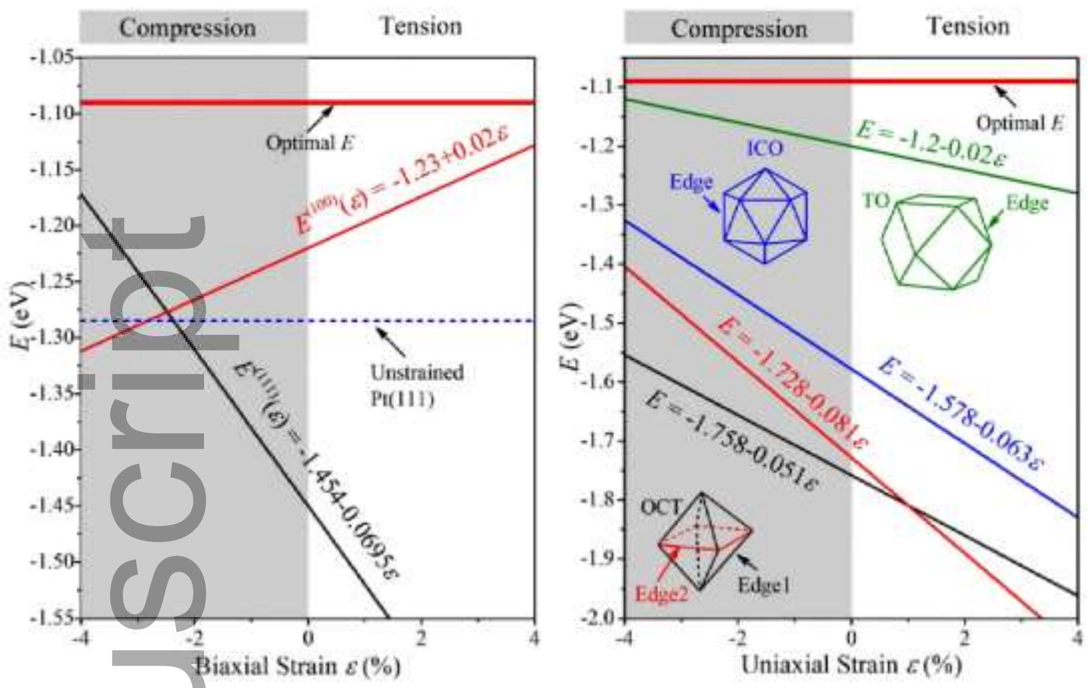

Figure 6. Oxygen adsorption energy (E) as a function of surface strain (ε) on different facets (left) and edges (right). The red solid and blue dashed horizontal lines represent the optimal E value for maximal ORR activity and the E value on unstrained Pt(111) surface, respectively. The insets of the right panel indicate the corresponding edges. Reproduced with permission.[155] Copyright 2017, American Chemical Society.

In addition to the compressive strain that could promotionally contribute the enhancement to the ORR performance, the tensile strain could also diminish the overlap of the wave functions and downshift the σ* antibonding states near the Fermi level. This could weaken the binding affinity of oxygen species to the surface atoms and accelerate the overall reaction rate.[156-160] Such ORR activity improvement on a tensile-strained surface was claimed by Huang and coworkers using a unique class of Pd−Pb@Pd core-shell nanosheets and nanocubes that they constructed with tensile strain on the (100) of both the top-Pd and edge-Pd surfaces.[161] The mass activities of the resultant Pd−Pb@Pd core-shell nanosheets and nanocubes were reported as 1.6- and 1.4-fold as high as those of the unshelled counterparts, respectively. Especially, the Pd−Pb@Pd core-shell nanosheets exhibit a mass activity of 0.57 A/mg_{Pd} at 0.90 V, which are 8.8 and 6.5 times as high as those of the commercial Pd/C and Pt/C, respectively. In a subsequent study, Zeng and coworkers reported the Pd@PdFe core−shell icosahedra with a three-atomic-layer tensile strained PdFe overlayer as a high-efficient and durable electrocatalyst toward ORR.[35] They showed 2.8-fold enhancement in mass activity in comparison with the commercial Pt/C catalyst in 0.1 M KOH solution, and this performance was superior to most of the non-Pt electrocatalysts (Figure 7a and 7b) reported previously. In this case, the volcano-type relationship was revealed with the maximal ORR performance at the Fe percentage of 9.0%, which can be generally understood based on the Sabatier principle. They further revealed that the synergistic coupling of tensile strain and alloy effects could optimize the binding strength with reaction intermediates, thus resulting in the maximum activity for ORR in alkaline media (Figure 7c).[35] As such, the tensile strain can be precisely controlled by optimizing the shell composition, like the previous case of PdAu hollow nanospheres with ultrathin Au-rich shells.[162]

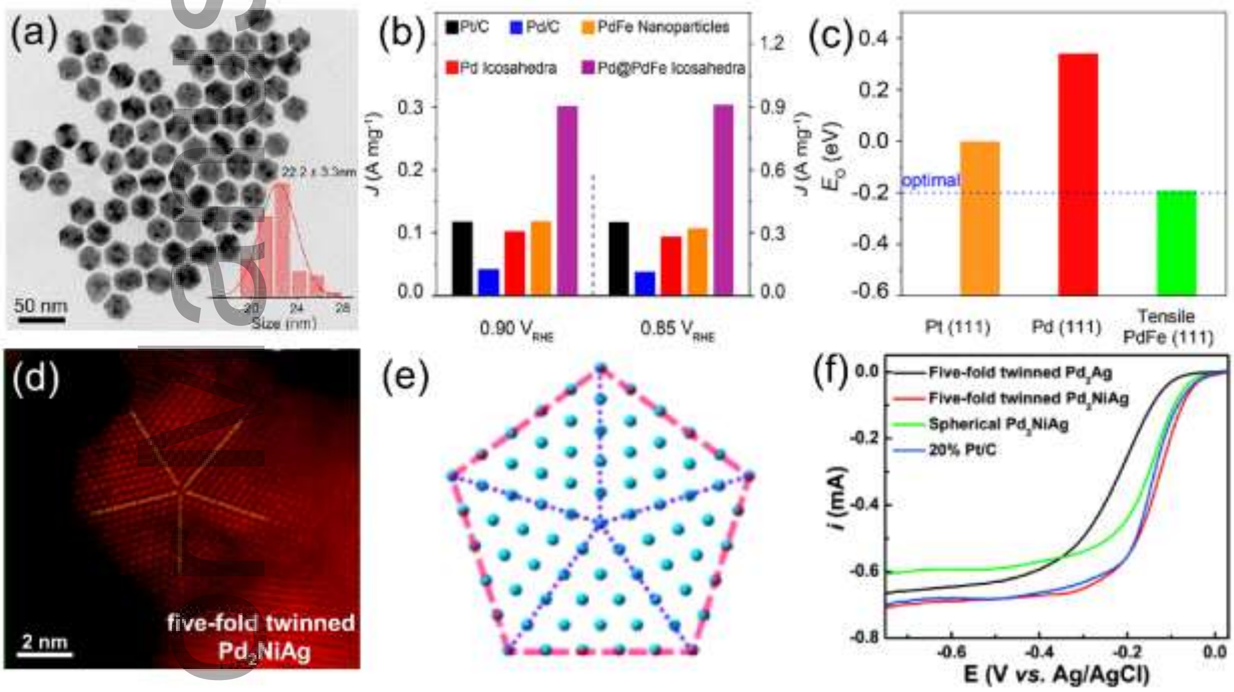

Figure 7. a) TEM image of Pd@PdFe core−shell icosahedra with the corresponding size distribution diagram as the inset. b) Mass activities of ORR calculated by normalizing the kinetic current densities to Pd loading mass of the catalysts on the electrode at 0.90 V_{RHE} and 0.85 V_{RHE}. c) The adsorption energy of adsorbed O atom (E_O) for Pt(111) surface, Pd(111) surface, and PdFe(111) surface with 2.0% tensile strain and Fe percentage of 8.3%. Note that the E_O for the pure Pt(111) surface is set as zero and the optimal E_O for ORR is about −0.2 eV. a-c) Reproduced with permission[35] and modified. Copyright 2020, American Chemical Society. d) HAADF image of Pd_2NiAg nanocrystals with five-fold twinning outlined by five dotted lines. e) Structural model for five-fold twinning consistent with the atomic projections in (d). f) ORR polarization curves in O_2-saturated 0.1 M KOH solution at a scan rate of 5 mV/s and rotation rate of 1600 rpm. d-f) Reproduced with permission.[163] Copyright 2015, American Chemical Society.

The lattice strain on the surface can be induced not only in core-shell structures but also in other nano-architectures, such as nanocrystals with twinned boundaries.[164, 165] It has been well-demonstrated that the twinned and non-twinned nanocrystals showed entirely different electrocatalytic behaviors in the typical face-centered cubic (*fcc*) structure. For instance, relative to the spherical Pd_2NiAg nanoparticles and the commercial Pt/C catalyst, five-fold twinned Pd_2NiAg nanocrystals with a Ni-terminated surface exhibited substantially enhanced electrocatalytic performance for ORR in alkaline media (Figure 7d-f).[163] Combining experimental observations with DFT calculations, Dai and coworkers reported that the surfaces of the five-fold twinned Pd_2NiAg nanocrystals show a particular valence electron density, where an optimal geometric arrangement of surface atoms greatly contributed to catalyzing ORR. Shortly, Huang and coworkers further revealed that the Pd_6Ni icosahedra display the highest activity and durability in 0.1 M KOH with a mass activity of 0.22 A mg_{Pd}^{-1}, as compared with PdNi icosahedra with different Ni contents and Pt/C catalyst.[166] Particularly, the presence of twin boundary and underlying Ni atoms with a specific content can cause the obvious shifting of the *d*-band center by weakening the interaction between the adsorbed O and Pd (111) surface, thus boosting the ORR activity. Altogether, controlling the surface strain of a Pd-based electrocatalyst could offer a novel and significant route for achieving enhanced ORR performance in alkaline media.

3.5 De-alloying

For a given alloy electrocatalyst, de-alloying has been generally considered as an effective and robust approach to regulating the surface electronic structure and the chemical composition by selectively removing one or more components, thus significantly tuning their electrocatalytic performance.[167-172] Typically, the removal of the less noble atoms from the topmost surface may effectively contribute to a formation of steps and kinks, where the coordinated numbers of noble atoms would increase accordingly, facilitating a surface diffusion of noble atoms and thus surface reconstruction. Relative to other approaches, the advantages of de-alloying are simple and high-yielding without involving the use of organic solvents. Solid core−shell and nanoporous structures with interconnected nanoscale skeletons and voids are often obtained using this method, which is particularly beneficial for the electrocatalytic process. Usually, the de-alloying approach might not be favorable for precise control of the composition since it is excessively sensitive to the experimental parameters. For example, Abruña and coworkers reported an electrochemical de-alloying strategy to significantly improve the ORR activity and stability of Pd/M□ (M□ = Ni and Mn) electrocatalysts in alkaline media through deliberately etching one component which is more active (Figure 8a).[61] Notably, after this electrochemical de-alloying, it was confirmed that the sample possesses a core-shell structure with a higher ratio of electrochemically active Pd on the surface. This benefits from an increase in the atomic utilization of active components (Figure 8b and 8c). However, the electrochemical de-alloying method may not be always favorable for the formation of core-shell structure, depending on the processing conditions such as the applied potential and the reaction time. Hall and coworkers utilized the electrochemical de-alloying approach for converting as-synthesized ordered intermetallic $PdBi_2$ to ordered intermetallic Pd_3Bi nanoparticles under ambient conditions (Figure 8d).[173] They identified that the formation of Pd_3Bi nanoparticles could mainly be attributed to the $PdBi_2$ with low melting point and low vacancy formation energies, which drives the facile removal of the Bi from the surface and interdiffusion of the constituent atoms. Importantly, the resultant Pd_3Bi nanoparticles exhibited more positive half-wave potential determined in O_2-saturated 0.1 M KOH solution (Figure 8e), delivered mass activity that was ~11 times and ~3.5 times as high as those of Pt/C and Pd/C, respectively, and demonstrated promising durability toward ORR in alkaline media (Figure 8f).

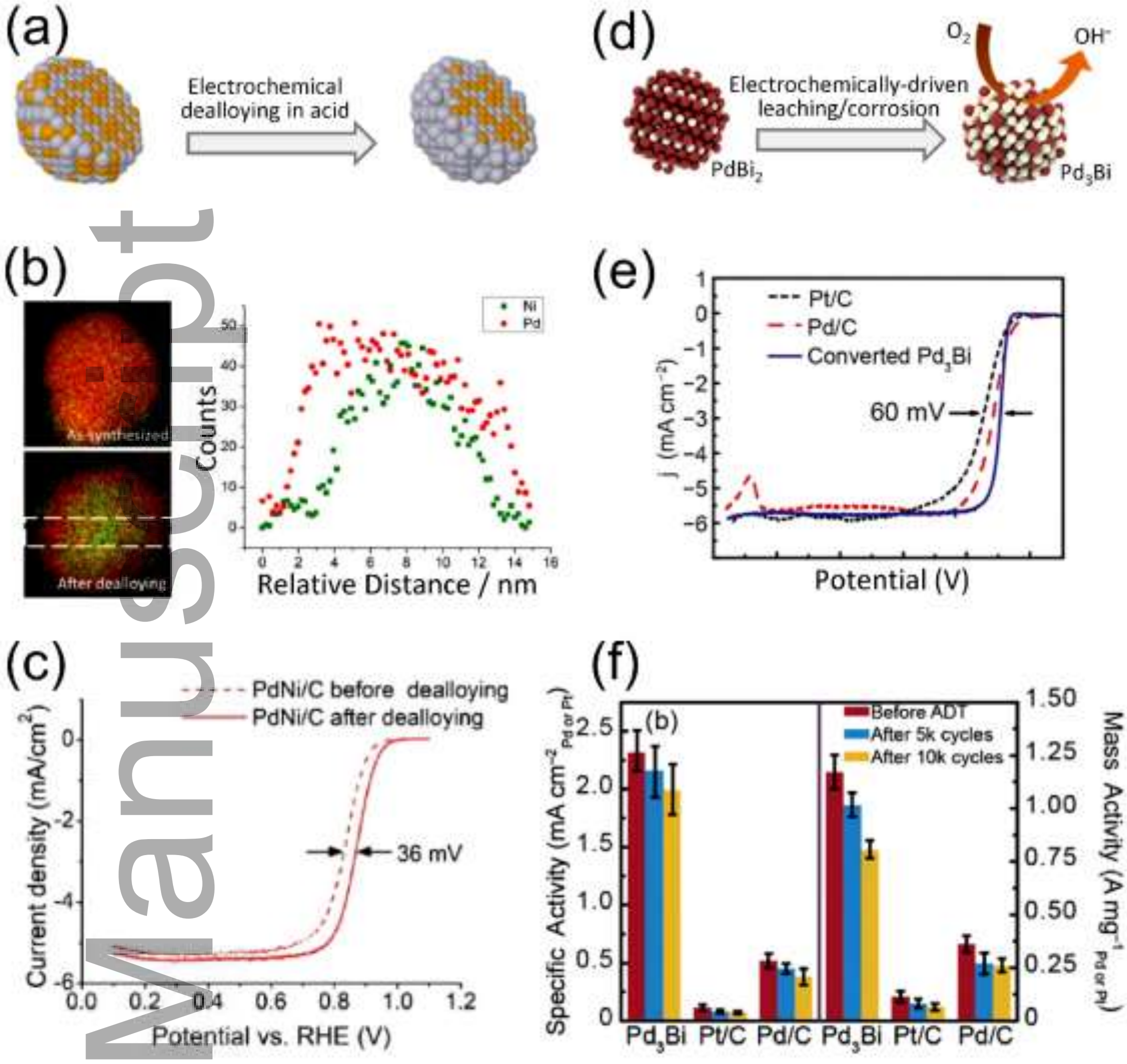

Figure 8. a) Schematic illustration of Pd/M (M = Ni, Mn) nanoparticles through the electrochemical de-alloying approach. b) EELS elemental composition maps of as-synthesized PdNi/C and after electrochemical de-alloying, and corresponding EELS elemental line scan of Pd and Ni derived from the white box in (b) from the EELS mapping. Note that the red color represents Pd is and the green color represents Ni. c) ORR polarization curves in O_2-saturated 0.1 M NaOH of PdNi/C before and after de-alloying at a sweep rate of 5 mV/s and rotation rate of 1600 rpm. a-c) Reproduced with permission[61] and modified, Copyright 2020, American Chemical Society. d) Schematic illustration of the synthesis of ordered intermetallic Pd_3Bi by an electrochemically induced phase transformation and ORR polarization curves of Pt/C, Pd/C, and converted Pd_3Bi in O_2-saturated 0.1 M KOH. Reproduced with permission[173] and modified. Copyright 2019, American Chemical Society.

Except for the electrochemical de-alloying approach, the chemical de-alloying approach was also generally utilized to synthesize Pd-based electrocatalysts with different structures using various chemical reagents including acids and alkalis for improving the ORR performance.[174-179] Cui and coworkers developed a one-step approach and prepared nanoporous PdCe nanocubes by selectively de-alloying ternary $Pd_{15}Ce_5Al_{80}$ alloy ribbons in 5 M NaOH solution for 48 h at 50 °C.[180] Supported by electrochemical evaluation and DFT calculations, they reported that alloying Pd with Ce could induce an obvious negative shift of the *d*-band center relative to that of Pd, which dramatically weakens its binding to O and thereby increases the intrinsic ORR activity of the PdCe alloy. Additionally, the morphology and microstructure of the final products could be affected by any of the synthetic parameters, including the type and concentration of chemicals, de-alloying temperature and time. Before this work, Zhang and coworkers also prepared a series of nanoporous alloys with different microstructures, compositions, and porosities by successively de-alloying a ternary alloy $Al_{75}Pd_{17.5}Au_{7.5}$ alloy in NaOH/HCl and HNO_3 aqueous solutions.[181] These nanoporous alloys with unique structures and compositions could be potentially served as promising candidates for ORR catalysts in alkaline media. In short, de-alloying has become a useful approach to strengthen the electrocatalytic performance by precisely manipulating the surface structure, composition, and strain.

In a remark, the aforementioned strategies are capable of being widely applied for delicately tuning the ORR performance of Pd-based electrocatalysts. These methods as well as their combinations can also significantly facilitate the understanding of structure–performance relationship and the intrinsic reaction mechanisms. To summarize these contributions clearly, some typical Pd-containing electrocatalysts together with their synthetic strategies and ORR activities in alkaline media are presented in Table 2. It is worth pointing out that, in some cases, it is vital to simultaneously couple multiple strategies in a practical syntheses system, ultimately resulting in extraordinary performance improvement. In addition, it seems that regulating the metal-support interaction in Pd-based hybrid catalysts has recently been demonstrated to be an effective strategy to advance their ORR performance,[58] and increasing interests begin to focus on the development of general and cost-saving strategies to enable gaining high-efficient ORR catalysts used in alkaline polymer electrolyte fuel cells (APEFC).

Table 2. Summary of the synthesis methods and ORR activities of some typical Pd-containing electrocatalysts reported previously in alkaline media.

Catalysts	Synthesis method	Electrolyte	Mass activity at 0.9 V (A mg_{Pd}^{-1})	Specific Activity at 0.9 V (mA cm_{Pd}^{-2})	Half-wave potential $E_{1/2}$ (V *vs.* RHE)	Reference
Ordered intermetallic Pd_3Pb	Phase control	0.1 M KOH	0.169	NA	0.92	[34]
Pd@PdFe core−shell icosahedra	Surface-strain control	0.1 M KOH	0.31	1.56	NA	[35]
Pd_3Pb ultrathin porous intermetallic nanosheets	Surface-strain control	0.1 M KOH	0.59	1.18	NA	[79]

Dendritic $Pd_{59}Cu_{30}Co_{11}$ nanoalloy	Surface-strain control	0.1 M KOH	0.38	0.9	0.91	[80]
$Pd_{17}Se_{15}$ nanoparticles	Phase control	0.1 M KOH	0.460	1.201	NA	[102]
Ordered PdCuCo nanoparticles	Phase control	0.1 M NaOH	0.13	NA	0.872	[103]
$L1_2$-ordered Pd_3Pb tripods	Phase control	0.1 M KOH	0.56	1.76	NA	[108]
Ordered intermetallic $Pd_{31}Bi_{12}$	Phase control	0.1 M KOH	NA	9.2	0.93	[109]
Monoclinic Pd_5Bi_2	Phase control	0.1 M KOH	2.05	NA	0.93	[29]
Pd−P nanoparticle	Heteroatom doping	0.1 M KOH	2.21	5.16	0.85	[124]
$Pd_{50}Cu_{50}$ thin films	Heteroatom doping	1 M KOH	0.13	2.3	0.886	[130]
Pd-B nanoparticles	Heteroatom doping	0.1 M KOH	2.38	4.13	0.86	[140]
B-Pd nanoparticles	Heteroatom doping	0.1 M KOH	0.97	1.27	NA	[143]
Ternary PdBP mesoporous nanospheres	Heteroatom doping	0.1 M KOH	1.45	2.45	0.92	[146]
AuCu@Pd core-shell nanoparticles	Surface-strain control	1 M KOH	1.781	1.08	NA	[154]
Tensile strained Pd_3Pb@Pd core-shell nanosheets	Surface-strain control	0.1 M KOH	0.574	1.31	NA	[161]
PdAu hollow nanospheres with Au- rich shells	Surface-strain control	0.1 M KOH	0.153	0.13	0.866	[162]
Pd_6Ni icosahedra	Surface-strain control	1 M KOH	0.22	0.66	NA	[166]
Ordered intermetallic Pd_3Bi nanoparticles	Phase control	0.1 M KOH	1.2	2.3	~0.95	[173]
Ni–Pd core–shell nanoparticles	Surface-strain control	0.1 M KOH	0.038	NA	0.86	[30]
Ordered intermetallic Pd_3Fe	Phase control	0.1 M KOH	0.0974	NA	~0.88	[107]
Nanoporous PdCe nanocubes	De-alloying	0.1 M KOH	0.078	NA	NA	[180]

4. Conclusions and Perspectives

In this review, we have elaborately outlined recent research advances on the exquisite design of cost-effective and high-performance Pd-based ORR electrocatalysts in alkaline fuel cells at the atomic level. Considerable progress has been made in the synthesis, characterization, and related evaluation for ORR in alkaline media. These developed approaches such as shape control, crystal phase exploration, heteroatom doping, surface strain engineering, and de-alloying have significantly boosted the ORR performance of many Pd-based electrocatalysts.

Despite these achievements, there still remains plenty of room for rationally designing Pd-based advanced electrocatalysts and for attaining deliberate synthesis of new electrocatalysts with high activity and remarkable long-term durability toward alkaline ORR. Currently, the mechanistic understanding of the controlled synthesis at the atomic or molecular level and thus establishing the fundamental correlation between the nanostructure and ORR performance are falling far behind the development of synthetic strategies in terms of empirical theory and insights. Specifically, inescapable and well-known issues often come with the irreproducibility of the synthesis and narrow applicability of the established approaches. As such, future development to address these issues should devote more efforts to exploiting *in-situ* techniques with high-resolution characterizations at the atomic-scale and quantitative assessment since these are crucial for deeply understanding the intrinsic reaction mechanisms. On this basis, simultaneously combining several approaches may be considered to be effective for greatly boosting the activity and durability of Pd-based ORR catalysts. Meanwhile, there is a considerable mismatch in assessing intrinsic catalytic activity and stability between rotating disk electrode (RDE) and membrane electrode assembly (MEA) techniques, mainly due to the obvious discrepancy in mass transport, catalyst layer thickness, operating temperature and pressure. To bridge this gap and contribute to fast screening high-efficient ORR catalysts, it is highly expected to develop novel evaluation techniques for fuel cells, such as floating electrode technique (FET) and thin-film gas diffusion electrode (GDE) technique.[182, 183] Additionally, the development of novel synthetic strategies is highly desirable and will be also essential for the precise control of Pd-based electrocatalysts. It is worth mentioning that solution-based approaches commonly use capping agents and stabilizers to regulate the growth of nanocrystals and avoid the nanocrystals aggregations. Many cleaning procedures including the post-synthesis treatment wouldn't effectively remove all of the capping agents and stabilizers that are absorbed on the surfaces of final products. Even trace amounts of the remaining chemicals on the catalyst surface would significantly hamper the performance toward ORR. Furthermore, the postcleaning process such as thermal annealing and plasmon treatment may also result in serious structural degradation. To avoid these issues, novel surfactant-free approaches for the synthesis of Pd-based electrocatalysts with revolutionary ORR performance in alkaline media are anticipated urgently.

Another unneglectable concern associated with the Pd-based electrocatalysts in alkaline media is their durability under harsh ORR conditions. In the preliminary laboratory studies, the testing period is typically in a range of ~10 to ~100 h. However, to meet the U.S. DOE target of 8000 h for practical applications, the stability of Pd-based electrocatalysts needs to be substantially increased. Moreover, relevant studies with respect to the degradation mechanisms of Pd-based electrocatalysts are still lacking. Perhaps, integration of operando spectroscopic measurements and computational simulations may offer a feasible strategy to probe the mechanistic origin, which can be also used to guide the strategic synthesis. Meanwhile, it has been discussed that the unstable carbon support in alkaline media could ultimately lead to the generation of metal carbonates on the interfaces between the catalyst and the support. As a result, the development of novel support with high stability for Pd-based electrocatalysts should be another milestone in this field.

Conflict of Interest

The authors declare no conflict of interest.

Keywords

Nanoscale design; Pd-based electrocatalysts; Oxygen reduction reaction (ORR); Alkaline media; Nanocrystals

Acknowledgments

M.Z. was primarily supported by the Center for Alkaline Based Energy Solutions (CABES), an Energy Frontier Research Center funded by the U.S. Department of Energy, Office of Science, Basic Energy Sciences at Binghamton University under award # DE-SC0019445. M.Z. was also partially supported by the National Science Foundation under award # DMR-1808383. Work done at Binghamton University was supported by S3IP as well.

Biographies

Ming Zhou received his B.S. and Ph.D. degrees in Chemical Engineering and Technology from Chongqing University in 2011 and 2017, respectively. He worked as a visiting graduate student in Prof. Younan Xia's group from 2014 to 2016. After obtained his Ph.D. degree in 2017, he started as a postdoctoral fellow at Nanyang Technological University under the supervision of Prof. Hua Zhang. In 2019, he joined Prof. Jiye Fang's group as a postdoctoral fellow at State University of New York at Binghamton. His research interests include the development of novel synthetic protocols for the shape-control synthesis of noble metal-based and spinel nanocrystals for applications in catalysis and renewable energy.

Jiangna Guo received her B.S. and M.S. degrees in Chemical Engineering and Technology from Chongqing University in 2012 and 2015, respectively. She joined the College of Chemistry and Chemical Engineering from Chongqing University in 2015, as a teacher in charge of undergraduate education. In 2018, she worked as a visiting scholar in Prof. Hua Zhang's group at Nanyang Technological University. She is currently pursuing a Ph.D. degree at Chongqing University. Her research interest includes the synthesis of nanomaterials for catalytic and sustainable energy applications.

Jiye Fang received his Ph.D. degree in Materials Science from National University of Singapore in 1999. He was a Postdoctoral Associate and subsequently Research Specialist from 1999 to 2002 at Advanced Materials Research Institute. He joined the Chemistry Department at University of New Orleans as an Assistant Professor in 2002, and then moved to State University of New York at Binghamton in 2006. He was an NSF CAREER award recipient. He is now the Professor of Chemistry and MSE at Binghamton. His current research interests include synthesis of shape-controlled nanocrystals, self-assembly and superstructure, lattice strain study on noble metal-based nanocrystals, advanced catalysts for fuel cell applications in acidic and alkaline media.

TOC

This review focuses on Palladium (Pd)-based electrocatalysts for the oxygen reduction reaction (ORR) in alkaline media. After a brief introduction and fundamental ORR mechanism overview, various strategies for delicately designing high-performance Pd-based catalysts are throughout discussed together with associated examples. Perspectives with challenges and new insights are further outlined, and some emerging research directions are also proposed.

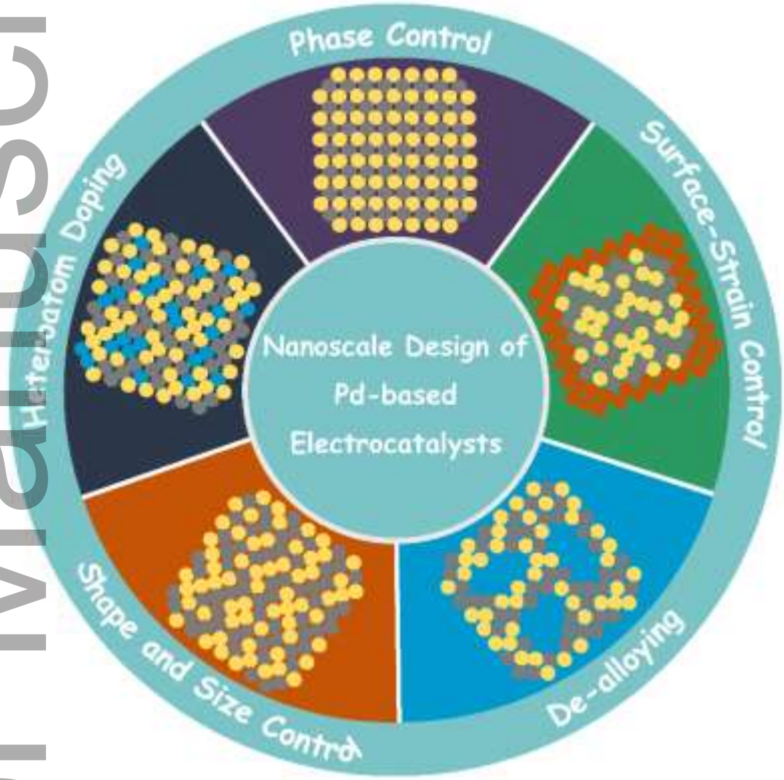

References

[1] M. K. Debe, *Nature* **2012**, *486*, 43.

[2] K. Kodama, T. Nagai, A. Kuwaki, R. Jinnouchi, Y. Morimoto, *Nat. Nanotechnol.* **2021**, *16*, 140.

[3] B. Pivovar, *Nat. Catal.* **2019**, *2*, 562.

[4] C.-Y. Wang, *Chem. Rev.* **2004**, *104*, 4727.

[5] M. Shao, Q. Chang, J.-P. Dodelet, R. Chenitz, *Chem. Rev.* **2016**, *116*, 3594.

[6] A. Kulkarni, S. Siahrostami, A. Patel, J. K. Nørskov, *Chem. Rev.* **2018**, *118*, 2302.

[7] W. Seh Zhi, J. Kibsgaard, F. Dickens Colin, I. Chorkendorff, K. Nørskov Jens, F. Jaramillo Thomas, *Science* **2017**, *355*, eaad4998.

[8] J. Jiang, W. Ding, W. Li, Z. Wei, *Chem.* **2020**, *6*, 431.

[9] Y. Wang, D. Wang, Y. Li, *SmartMat* **2021**, *2*, 56.

[10] X. Ren, Q. Lv, L. Liu, B. Liu, Y. Wang, A. Liu, G. Wu, *Sustainable Energy Fuels* **2020**, *4*, 15.

[11] R. Stamenkovic Vojislav, B. Fowler, S. Mun Bongjin, G. Wang, N. Ross Philip, A. Lucas Christopher, M. Marković Nenad, *Science* **2007**, *315*, 493.

[12] Z. Ma, Z. P. Cano, A. Yu, Z. Chen, G. Jiang, X. Fu, L. Yang, T. Wu, Z. Bai, J. Lu, *Angew. Chem. Int. Ed.* **2020**, *59*, 18334.

[13] J. Zhang, H. Yang, J. Fang, S. Zou, *Nano Lett.* **2010**, *10*, 638.

[14] Q. Gao, M.-R. Gao, J.-W. Liu, M.-Y. Chen, C.-H. Cui, H.-H. Li, S.-H. Yu, *Nanoscale* **2013**, *5*, 3202.

[15] E. Antolini, *Energy Environ. Sci.* **2009**, *2*, 915.

[16] H. Zhang, X. Qiu, Y. Chen, S. Wang, S. E. Skrabalak, Y. Tang, *Small* **2020**, *16*, 1906026.

[17] J. Sanabria-Chinchilla, K. Asazawa, T. Sakamoto, K. Yamada, H. Tanaka, P. Strasser, *J. Am. Chem. Soc.* **2011**, *133*, 5425.

[18] J. K. Dombrovskis, H. Y. Jeong, K. Fossum, O. Terasaki, A. E. C. Palmqvist, *Chem. Mater.* **2013**, *25*, 856.

[19] P. D. Tran, A. Morozan, S. Archambault, J. Heidkamp, P. Chenevier, H. Dau, M. Fontecave, A. Martinent, B. Jousselme, V. Artero, *Chem. Sci.* **2015**, *6*, 2050.

[20] Y. Zhan, F. Xie, H. Zhang, Z. Lin, J. Huang, W. Zhang, X. Sun, Y. Zhang, J. Chen, H. Meng, *J. Electrochem. Soc.* **2018**, *165*, J3008.

[21] X. Zhou, J. Qiao, L. Yang, J. Zhang, *Adv. Energy Mater.* **2014**, *4*, 1301523.

[22] B. Li, J. Prakash, *Electrochem. Commun.* **2009**, *11*, 1162.

[23] D. A. Slanac, W. G. Hardin, K. P. Johnston, K. J. Stevenson, *J. Am. Chem. Soc.* **2012**, *134*, 9812.

[24] X. Huang, A. J. Shumski, X. Zhang, C. W. Li, *J. Am. Chem. Soc.* **2018**, *140*, 8918.

[25] J. A. Zamora Zeledón, M. B. Stevens, G. T. K. K. Gunasooriya, A. Gallo, A. T. Landers, M. E. Kreider, C. Hahn, J. K. Nørskov, T. F. Jaramillo, *Nat. Commun.* **2021**, *12*, 620.

[26] D. Wang, S. Liu, J. Wang, R. Lin, M. Kawasaki, E. Rus, K. E. Silberstein, M. A. Lowe, F. Lin, D. Nordlund, H. Liu, D. A. Muller, H. L. Xin, H. D. Abruña, *Nat. Commun.* **2016**, *7*, 11941.

[27] X. Ge, A. Sumboja, D. Wuu, T. An, B. Li, F. W. T. Goh, T. S. A. Hor, Y. Zong, Z. Liu, *ACS Catal.* **2015**, *5*, 4643.

[28] M. V. Castegnaro, W. J. Paschoalino, M. R. Fernandes, B. Balke, M. C. M. Alves, E. A. Ticianelli, J. Morais, *Langmuir* **2017**, *33*, 2734.

[29] M. Zhou, J. Guo, B. Zhao, C. Li, L. Zhang, J. Fang, *J. Am. Chem. Soc.* **2021**, *143*, 15891.

[30] J. Jiang, H. Gao, S. Lu, X. Zhang, C.-Y. Wang, W.-K. Wang, H.-Q. Yu, *J. Mater. Chem. A* **2017**, *5*, 9233.

[31] W. Xiao, M. A. Liutheviciene Cordeiro, M. Gong, L. Han, J. Wang, C. Bian, J. Zhu, H. L. Xin, D. Wang, *J. Mater. Chem. A* **2017**, *5*, 9867.

[32] M. Luo, S. Guo, *Nat. Rev. Mater.* **2017**, *2*, 17059.

[33] Q. Gao, Y.-M. Ju, D. An, M.-R. Gao, C.-H. Cui, J.-W. Liu, H.-P. Cong, S.-H. Yu, *ChemSusChem* **2013**, *6*, 1878.

[34] Z. Cui, H. Chen, M. Zhao, F. J. DiSalvo, *Nano Lett.* **2016**, *16*, 2560.

[35] X. Li, X. Li, C. Liu, H. Huang, P. Gao, F. Ahmad, L. Luo, Y. Ye, Z. Geng, G. Wang, R. Si, C. Ma, J. Yang, J. Zeng, *Nano Lett.* **2020**, *20*, 1403.

[36] H. Erikson, A. Sarapuu, J. Solla-Gullón, K. Tammeveski, *J. Electroanal. Chem.* **2016**, *780*, 327.

[37] H. Xu, H. Shang, C. Wang, Y. Du, *Small* **2021**, *17*, 2005092.

[38] T. Wang, A. Chutia, D. J. L. Brett, P. R. Shearing, G. He, G. Chai, I. P. Parkin, *Energy Environ. Sci.* **2021**, *14*, 2639.

[39] F. D. Sanij, P. Balakrishnan, P. Leung, A. Shah, H. Su, Q. Xu, *Int. J. Hydrogen Energy* **2021**, *46*, 14596.

[40] J. Fan, H. Du, Y. Zhao, Q. Wang, Y. Liu, D. Li, J. Feng, *ACS Catal.* **2020**, *10*, 13560.

[41] L. Zhang, Q. Chang, H. Chen, M. Shao, *Nano Energy* **2016**, *29*, 198.

[42] H. Erikson, A. Sarapuu, N. Alexeyeva, K. Tammeveski, J. Solla-Gullón, J. M. Feliu, *Electrochim. Acta* **2012**, *59*, 329.

[43] M. Shao, *J. Power Sources* **2011**, *196*, 2433.

[44] Y. Nie, L. Li, Z. Wei, *Chem. Soc. Rev.* **2015**, *44*, 2168.

[45] Z. Zhao, C. Chen, Z. Liu, J. Huang, M. Wu, H. Liu, Y. Li, Y. Huang, *Adv. Mater.* **2019**, *31*, 1808115.

[46] A. Holewinski, S. Linic, *J. Electrochem. Soc.* **2012**, *159*, H864.

[47] L. Ou, S. Chen, *J. Phys. Chem. C* **2013**, *117*, 1342.

[48] Y. Sha, T. H. Yu, B. V. Merinov, P. Shirvanian, W. A. Goddard, *J. Phys. Chem. Lett.* **2011**, *2*, 572.

[49] L. Ou, *J. Chem.* **2015**, *2015*, 932616.

[50] J. K. Nørskov, J. Rossmeisl, A. Logadottir, L. Lindqvist, J. R. Kitchin, T. Bligaard, H. Jónsson, *J. Phys. Chem. B* **2004**, *108*, 17886.

[51] M. H. Shao, T. Huang, P. Liu, J. Zhang, K. Sasaki, M. B. Vukmirovic, R. R. Adzic, *Langmuir* **2006**, *22*, 10409.

[52] N. A. Anastasijević, V. Vesović, R. R. Adžić, *J. Electroanal. Chem. Interfacial Electrochem.* **1987**, *229*, 317.

[53] K.-L. Huang, Z.-T. Liu, C.-L. Lee, *Electrochim. Acta* **2015**, *157*, 78.

[54] I. Srejic, Z. Rakocevic, M. Nenadovic, S. Strbac, *Electrochim. Acta* **2015**, *169*, 22.

[55] T. Mittermeier, A. Weiß, H. A. Gasteiger, F. Hasché, *J. Electrochem. Soc.* **2017**, *164*, F1081.

[56] J. Rossmeisl, J. K. Nørskov, *Surf. Sci.* **2008**, *602*, 2337.

[57] Y. Xie, C. Li, E. Castillo, J. Fang, N. Dimitrov, *Electrochim. Acta* **2021**, *385*, 138306.

[58] Y. Lu, Y. Jiang, X. Gao, X. Wang, W. Chen, *J. Am. Chem. Soc.* **2014**, *136*, 11687.

[59] G. Bampos, L. Sygellou, S. Bebelis, *Catal. Today* **2020**, *355*, 685.

[60] G. Bampos, S. Bebelis, D. I. Kondarides, X. Verykios, *Top. Catal.* **2017**, *60*, 1260.

[61] X. Lu, M. Ahmadi, F. J. DiSalvo, H. D. Abruña, *ACS Catal.* **2020**, *10*, 5891.

[62] M. Lüsi, H. Erikson, M. Merisalu, M. Rähn, V. Sammelselg, K. Tammeveski, *J. Electroanal. Chem.* **2019**, *834*, 223.

[63] T. Kar, R. Devivaraprasad, B. Bera, R. Ramesh, M. Neergat, *Electrochim. Acta* **2016**, *191*, 81.

[64] J. Shi, J. Wang, Y. Chen, Y. Sun, B. Liu, Y. Fan, *Journal of Physics: Materials* **2020**, *4*, 014002.

[65] L. E. Betancourt, A. Rojas-Pérez, I. Orozco, A. I. Frenkel, Y. Li, K. Sasaki, S. D. Senanayake, C. R. Cabrera, *ACS Applied Energy Materials* **2020**, *3*, 2342.

[66] A. M. Henning, J. Watt, P. J. Miedziak, S. Cheong, M. Santonastaso, M. Song, Y. Takeda, A. I. Kirkland, S. H. Taylor, R. D. Tilley, *Angew. Chem. Int. Ed.* **2013**, *52*, 1477.

[67] J. Gu, Y.-W. Zhang, F. Tao, *Chem. Soc. Rev.* **2012**, *41*, 8050.

[68] B. Lim, M. Jiang, J. Tao, P. H. C. Camargo, Y. Zhu, Y. Xia, *Adv. Funct. Mater.* **2009**, *19*, 189.

[69] Y. Xia, Y. Xiong, B. Lim, S. E. Skrabalak, *Angew. Chem. Int. Ed.* **2009**, *48*, 60.

[70] L. Zhang, Z. Xie, J. Gong, *Chem. Soc. Rev.* **2016**, *45*, 3916.

[71] A. Chen, C. Ostrom, *Chem. Rev.* **2015**, *115*, 11999.

[72] S. Ahmadi Temer, L. Wang Zhong, C. Green Travis, A. Henglein, A. El-Sayed Mostafa, *Science* **1996**, *272*, 1924.

[73] S. Liu, H. Tao, L. Zeng, Q. Liu, Z. Xu, Q. Liu, J.-L. Luo, *J. Am. Chem. Soc.* **2017**, *139*, 2160.

[74] D. Xu, Z. Liu, H. Yang, Q. Liu, J. Zhang, J. Fang, S. Zou, K. Sun, *Angew. Chem. Int. Ed.* **2009**, *48*, 4217.

[75] K. D. Gilroy, A. Ruditskiy, H.-C. Peng, D. Qin, Y. Xia, *Chem. Rev.* **2016**, *116*, 10414.

[76] C. Zhu, S. Guo, S. Dong, *Adv. Mater.* **2012**, *24*, 2326.

[77] M. Zhou, H. Wang, M. Vara, Z. D. Hood, M. Luo, T.-H. Yang, S. Bao, M. Chi, P. Xiao, Y. Zhang, Y. Xia, *J. Am. Chem. Soc.* **2016**, *138*, 12263.

[78] M. Luo, Z. Zhao, Y. Zhang, Y. Sun, Y. Xing, F. Lv, Y. Yang, X. Zhang, S. Hwang, Y. Qin, J.-Y. Ma, F. Lin, D. Su, G. Lu, S. Guo, *Nature* **2019**, *574*, 81.

[79] J. Guo, L. Gao, X. Tan, Y. Yuan, J. Kim, Y. Wang, H. Wang, Y.-J. Zeng, S.-I. Choi, S. C. Smith, H. Huang, *Angew. Chem. Int. Ed.* **2021**, *60*, 10942.

[80] C. Li, Q. Yuan, B. Ni, T. He, S. Zhang, Y. Long, L. Gu, X. Wang, *Nat. Commun.* **2018**, *9*, 3702.

[81] Y. Zuo, D. Rao, S. Li, T. Li, G. Zhu, S. Chen, L. Song, Y. Chai, H. Han, *Adv. Mater.* **2018**, *30*, 1704171.

[82] B. Lim, M. Jiang, H. C. Camargo Pedro, C. Cho Eun, J. Tao, X. Lu, Y. Zhu, Y. Xia, *Science* **2009**, *324*, 1302.

[83] Y. Qi, J. Wu, H. Zhang, Y. Jiang, C. Jin, M. Fu, H. Yang, D. Yang, *Nanoscale* **2014**, *6*, 7012.

[84] J. T. L. Gamler, K. Shin, H. M. Ashberry, Y. Chen, S. L. A. Bueno, Y. Tang, G. Henkelman, S. E. Skrabalak, *Nanoscale* **2020**, *12*, 2532.

[85] H.-C. Li, Y.-J. Zhang, X. Hu, W.-J. Liu, J.-J. Chen, H.-Q. Yu, *Adv. Energy Mater.* **2018**, *8*, 1702734.

[86] Y. Lu, Y. Jiang, W. Chen, *Nano Energy* **2013**, *2*, 836.

[87] S. Luo, M. Tang, X. Wu, Y. Ou, Z. Wang, N. Jian, X. Li, Y. Lin, Y. Yan, J. Huang, H. Zhang, D. Yang, *CrystEngComm* **2019**, *21*, 290.

[88] C. Koenigsmann, A. C. Santulli, E. Sutter, S. S. Wong, *ACS Nano* **2011**, *5*, 7471.

[89] A. Anastasopoulos, J. C. Davies, L. Hannah, B. E. Hayden, C. E. Lee, C. Milhano, C. Mormiche, L. Offin, *ChemSusChem* **2013**, *6*, 1973.

[90] Y. Wang, F.-L. Hu, Y. Mi, C. Yan, S. Zhao, *Chem. Eng. J.* **2021**, *406*, 127135.

[91] C. Zhu, S. Fu, Q. Shi, D. Du, Y. Lin, *Angew. Chem. Int. Ed.* **2017**, *56*, 13944.

[92] Q. Zhang, J. Guan, *Adv. Funct. Mater.* **2020**, *30*, 2000768.

[93] J. Hu, W. Liu, C. Xin, J. Guo, X. Cheng, J. Wei, C. Hao, G. Zhang, Y. Shi, *J. Mater. Chem. A* **2021**, *9*, 24803.

[94] Q. Liu, Y. Li, L. Zheng, J. Shang, X. Liu, R. Yu, J. Shui, *Adv. Energy Mater.* **2020**, *10*, 2000689.

[95] S. Ji, Y. Chen, X. Wang, Z. Zhang, D. Wang, Y. Li, *Chem. Rev.* **2020**, *120*, 11900.

[96] C. Wan, X. Duan, Y. Huang, *Adv. Energy Mater.* **2020**, *10*, 1903815.

[97] R. Arrigo, M. E. Schuster, Z. Xie, Y. Yi, G. Wowsnick, L. L. Sun, K. E. Hermann, M. Friedrich, P. Kast, M. Hävecker, A. Knop-Gericke, R. Schlögl, *ACS Catal.* **2015**, *5*, 2740.

[98] Q. Liu, Y. Peng, Q. Li, T. He, D. Morris, F. Nichols, R. Mercado, P. Zhang, S. Chen, *ACS Appl. Mater. Interfaces* **2020**, *12*, 17641.

[99] W. Xiang, Y. Zhao, Z. Jiang, X. Li, H. Zhang, Y. Sun, Z. Ning, F. Du, P. Gao, J. Qian, K. Kato, M. Yamauchi, Y. Sun, *J. Mater. Chem. A* **2018**, *6*, 23366.

[100] Z. Fan, H. Zhang, *Chem. Soc. Rev.* **2016**, *45*, 63.

[101] Y. Chen, Z. Fan, Z. Luo, X. Liu, Z. Lai, B. Li, Y. Zong, L. Gu, H. Zhang, *Adv. Mater.* **2017**, *29*, 1701331.

[102] Z. Yu, S. Xu, Y. Feng, C. Yang, Q. Yao, Q. Shao, Y.-f. Li, X. Huang, *Nano Lett.* **2021**, *21*, 3805.

[103] K. Jiang, P. Wang, S. Guo, X. Zhang, X. Shen, G. Lu, D. Su, X. Huang, *Angew. Chem. Int. Ed.* **2016**, *55*, 9030.

[104] J. Li, S. Sun, *Acc. Chem. Res.* **2019**, *52*, 2015.

[105] Y. Yan, J. S. Du, K. D. Gilroy, D. Yang, Y. Xia, H. Zhang, *Adv. Mater.* **2017**, *29*, 1605997.

[106] M. Zhou, C. Li, J. Fang, *Chem. Rev.* **2021**, *121*, 736.

[107] Z. Cui, L. Li, A. Manthiram, J. B. Goodenough, *J. Am. Chem. Soc.* **2015**, *137*, 7278.

[108] L. Bu, Q. Shao, Y. Pi, J. Yao, M. Luo, J. Lang, S. Hwang, H. Xin, B. Huang, J. Guo, D. Su, S. Guo, X. Huang, *Chem.* **2018**, *4*, 359.

[109] Y. Wang, D. Sun, T. Chowdhury, J. S. Wagner, T. J. Kempa, A. S. Hall, *J. Am. Chem. Soc.* **2019**, *141*, 2342.

[110] W. Xiao, W. Lei, M. Gong, H. L. Xin, D. Wang, *ACS Catal.* **2018**, *8*, 3237.

[111] S. Maksimuk, S. Yang, Z. Peng, H. Yang, *J. Am. Chem. Soc.* **2007**, *129*, 8684.

[112] D. Wang, H. L. Xin, R. Hovden, H. Wang, Y. Yu, D. A. Muller, F. J. DiSalvo, H. D. Abruña, *Nat. Mater.* **2013**, *12*, 81.

[113] Y. Qiu, L. Xin, Y. Li, I. T. McCrum, F. Guo, T. Ma, Y. Ren, Q. Liu, L. Zhou, S. Gu, M. J. Janik, W. Li, *J. Am. Chem. Soc.* **2018**, *140*, 16580.

[114] Z. Cao, Q. Chen, J. Zhang, H. Li, Y. Jiang, S. Shen, G. Fu, B.-a. Lu, Z. Xie, L. Zheng, *Nat. Commun.* **2017**, *8*, 15131.

[115] Z. Li, X. Lu, J. Teng, Y. Zhou, W. Zhuang, *Nanoscale* **2021**, *13*, 11314.

[116] B. Jiang, X.-G. Zhang, K. Jiang, D.-Y. Wu, W.-B. Cai, *J. Am. Chem. Soc.* **2018**, *140*, 2880.

[117] R. Jiang, D. T. Tran, J. P. McClure, D. Chu, *ACS Catal.* **2014**, *4*, 2577.

[118] F. Gao, Y. Zhang, F. Ren, Y. Shiraishi, Y. Du, *Adv. Funct. Mater.* **2020**, *30*, 2000255.

[119] T. L. Tan, L.-L. Wang, D. D. Johnson, K. Bai, *Nano Lett.* **2012**, *12*, 4875.

[120] L. Chen, L. Lu, H. Zhu, Y. Chen, Y. Huang, Y. Li, L. Wang, *Nat. Commun.* **2017**, *8*, 14136.

[121] X. Bai, W. Chen, C. Zhao, S. Li, Y. Song, R. Ge, W. Wei, Y. Sun, *Angew. Chem. Int. Ed.* **2017**, *56*, 12219.

[122] L. Y. Chen, N. Chen, Y. Hou, Z. C. Wang, S. H. Lv, T. Fujita, J. H. Jiang, A. Hirata, M. W. Chen, *ACS Catal.* **2013**, *3*, 1220.

[123] Y. Liu, M. Chi, V. Mazumder, K. L. More, S. Soled, J. D. Henao, S. Sun, *Chem. Mater.* **2011**, *23*, 4199.

[124] K. C. Poon, D. C. L. Tan, T. D. T. Vo, B. Khezri, H. Su, R. D. Webster, H. Sato, *J. Am. Chem. Soc.* **2014**, *136*, 5217.

[125] H. Wang, W. Luo, L. Zhu, Z. Zhao, B. E, W. Tu, X. Ke, M. Sui, C. Chen, Q. Chen, Y. Li, Y. Huang, *Adv. Funct. Mater.* **2018**, *28*, 1707219.

[126] Y. Sun, X. Zhang, M. Luo, X. Chen, L. Wang, Y. Li, M. Li, Y. Qin, C. Li, N. Xu, G. Lu, P. Gao, S. Guo, *Adv. Mater.* **2018**, *30*, 1802136.

[127] W. Jiao, C. Chen, W. You, X. Zhao, J. Zhang, Y. Feng, P. Wang, R. Che, *Adv. Energy Mater.* **2020**, *10*, 1904072.

[128] K. A. Kuttiyiel, K. Sasaki, D. Su, L. Wu, Y. Zhu, R. R. Adzic, *Nat. Commun.* **2014**, *5*, 5185.

[129] M. Wang, W. Zhang, J. Wang, D. Wexler, S. D. Poynton, R. C. T. Slade, H. Liu, B. Winther-Jensen, R. Kerr, D. Shi, J. Chen, *ACS Appl. Mater. Interfaces* **2013**, *5*, 12708.

[130] Y. Yang, G. Chen, R. Zeng, A. M. Villarino, F. J. DiSalvo, R. B. van Dover, H. D. Abruña, *J. Am. Chem. Soc.* **2020**, *142*, 3980.

[131] W. Tang, L. Zhang, G. Henkelman, *J. Phys. Chem. Lett.* **2011**, *2*, 1328.

[132] M. Wang, X. Qin, K. Jiang, Y. Dong, M. Shao, W.-B. Cai, *J. Phys. Chem. C* **2017**, *121*, 3416.

[133] C. Zhang, S. Yu, Y. Xie, W. Zhang, K. Zheng, N. E. Drewett, S. J. Yoo, Z. Wang, L. Shao, H. Tian, J.-G. Kim, W. Zheng, *Carbon* **2019**, *149*, 370.

[134] T. Chen, C. Foo, S. C. Edman Tsang, *Chem. Sci.* **2021**, *12*, 517.

[135] Z. Zhao, X. Huang, M. Li, G. Wang, C. Lee, E. Zhu, X. Duan, Y. Huang, *J. Am. Chem. Soc.* **2015**, *137*, 15672.

[136] L. Bu, X. Zhu, Y. Zhu, C. Cheng, Y. Li, Q. Shao, L. Zhang, X. Huang, *CCS Chem.* **2020**, *3*, 1972.

[137] Y. Lu, J. Wang, Y. Peng, A. Fisher, X. Wang, *Adv. Energy Mater.* **2017**, *7*, 1700919.

[138] J. Fan, J. Wu, X. Cui, L. Gu, Q. Zhang, F. Meng, B.-H. Lei, D. J. Singh, W. Zheng, *J. Am. Chem. Soc.* **2020**, *142*, 3645.

[139] J. Fan, X. Cui, S. Yu, L. Gu, Q. Zhang, F. Meng, Z. Peng, L. Ma, J.-Y. Ma, K. Qi, Q. Bao, W. Zheng, *ACS Nano* **2019**, *13*, 12987.

[140] T. T. Vo Doan, J. Wang, K. C. Poon, D. C. L. Tan, B. Khezri, R. D. Webster, H. Su, H. Sato, *Angew. Chem. Int. Ed.* **2016**, *55*, 6842.

[141] T.-W. Jiang, Y.-W. Zhou, X.-Y. Ma, X. Qin, H. Li, C. Ding, B. Jiang, K. Jiang, W.-B. Cai, *ACS Catal.* **2021**, *11*, 840.

[142] L. Chen, L.-R. Zhang, L.-Y. Yao, Y.-H. Fang, L. He, G.-F. Wei, Z.-P. Liu, *Energy Environ. Sci.* **2019**, *12*, 3099.

[143] J. Li, J. Chen, Q. Wang, W.-B. Cai, S. Chen, *Chem. Mater.* **2017**, *29*, 10060.

[144] J. Zhang, L. Wu, L. Xu, D. Sun, H. Sun, Y. Tang, *Nanoscale* **2021**, *13*, 16052.

[145] H. Lv, Y. Wang, D. Xu, B. Liu, *Nano Res.* **2021**, *14*, 3274.

[146] H. Lv, D. Xu, L. Sun, J. Henzie, S. L. Suib, Y. Yamauchi, B. Liu, *ACS Nano* **2019**, *13*, 12052.

[147] M. Shao, P. Liu, J. Zhang, R. Adzic, *J. Phys. Chem. B* **2007**, *111*, 6772.

[148] B. T. Sneed, C. N. Brodsky, C.-H. Kuo, L. K. Lamontagne, Y. Jiang, Y. Wang, F. Tao, W. Huang, C.-K. Tsung, *J. Am. Chem. Soc.* **2013**, *135*, 14691.

[149] B. You, M. T. Tang, C. Tsai, F. Abild-Pedersen, X. Zheng, H. Li, *Adv. Mater.* **2019**, *31*, 1807001.

[150] C.-H. Kuo, L. K. Lamontagne, C. N. Brodsky, L.-Y. Chou, J. Zhuang, B. T. Sneed, M. K. Sheehan, C.-K. Tsung, *ChemSusChem* **2013**, *6*, 1993.

[151] L. Bu, N. Zhang, S. Guo, X. Zhang, J. Li, J. Yao, T. Wu, G. Lu, J.-Y. Ma, D. Su, X. Huang, *Science* **2016**, *354*, 1410.

[152] T. Wu, M. Sun, B. Huang, *Angew. Chem. Int. Ed.* **2021**, *60*, 22996.

[153] S. Guo, X. Zhang, W. Zhu, K. He, D. Su, A. Mendoza-Garcia, S. F. Ho, G. Lu, S. Sun, *J. Am. Chem. Soc.* **2014**, *136*, 15026.

[154] G. Wang, J. Guan, L. Xiao, B. Huang, N. Wu, J. Lu, L. Zhuang, *Nano Energy* **2016**, *29*, 268.

[155] Z. Chen, X. Zhang, G. Lu, *J. Phys. Chem. C* **2017**, *121*, 1964.

[156] E. E. Benson, M.-A. Ha, B. A. Gregg, J. van de Lagemaat, N. R. Neale, D. Svedruzic, *Sci. Rep.* **2019**, *9*, 15906.

[157] J. Wei, H.-L. Ya, S.-N. Qin, H. Zhang, Z.-Q. Tian, J.-F. Li, *J. Electroanal. Chem.* **2021**, *896*, 115205.

[158] T. Ling, M. Jaroniec, S.-Z. Qiao, *Adv. Mater.* **2020**, *32*, 2001866.

[159] D. Zhou, S. Wang, Y. Jia, X. Xiong, H. Yang, S. Liu, J. Tang, J. Zhang, D. Liu, L. Zheng, Y. Kuang, X. Sun, B. Liu, *Angew. Chem. Int. Ed.* **2019**, *58*, 736.

[160] J. Zhang, M. B. Vukmirovic, Y. Xu, M. Mavrikakis, R. R. Adzic, *Angew. Chem. Int. Ed.* **2005**, *44*, 2132.

[161] C. Tang, N. Zhang, Y. Ji, Q. Shao, Y. Li, X. Xiao, X. Huang, *Nano Lett.* **2019**, *19*, 1336.

[162] W. Jiao, C. Chen, W. You, G. Chen, S. Xue, J. Zhang, J. Liu, Y. Feng, P. Wang, Y. Wang, H. Wen, R. Che, *Appl. Catal., B* **2020**, *262*, 118298.

[163] S. Liu, Q. Zhang, Y. Li, M. Han, L. Gu, C. Nan, J. Bao, Z. Dai, *J. Am. Chem. Soc.* **2015**, *137*, 2820.

[164] A.-X. Yin, X.-Q. Min, W. Zhu, H.-S. Wu, Y.-W. Zhang, C.-H. Yan, *Chem. Commun.* **2012**, *48*, 543.

[165] M. Song, G. Zhou, N. Lu, J. Lee, E. Nakouzi, H. Wang, D. Li, *Science* **2020**, *367*, 40.

[166] Y. Feng, Q. Shao, Y. Ji, X. Cui, Y. Li, X. Zhu, X. Huang, *Sci. Adv.* **2018**, *4*, eaap8817.

[167] S. Koh, P. Strasser, *J. Am. Chem. Soc.* **2007**, *129*, 12624.

[168] K. C. Neyerlin, R. Srivastava, C. Yu, P. Strasser, *J. Power Sources* **2009**, *186*, 261.

[169] P. Strasser, S. Kühl, *Nano Energy* **2016**, *29*, 166.

[170] R. Srivastava, P. Mani, N. Hahn, P. Strasser, *Angew. Chem. Int. Ed.* **2007**, *46*, 8988.

[171] F.-J. Lai, W.-N. Su, L. S. Sarma, D.-G. Liu, C.-A. Hsieh, J.-F. Lee, B.-J. Hwang, *Chem. Eur. J.* **2010**, *16*, 4602.

[172] J. Wang, F. Chen, Y. Jin, Y. Lei, R. L. Johnston, *Adv. Funct. Mater.* **2017**, *27*, 1700260.

[173] D. Sun, Y. Wang, K. J. T. Livi, C. Wang, R. Luo, Z. Zhang, H. Alghamdi, C. Li, F. An, B. Gaskey, T. Mueller, A. S. Hall, *ACS Nano* **2019**, *13*, 10818.

[174] X. Chen, C. Si, Y. Wang, Y. Ding, Z. Zhang, *Nano Res.* **2016**, *9*, 1831.

[175] C. Xu, Y. Liu, Q. Hao, H. Duan, *J. Mater. Chem. A* **2013**, *1*, 13542.

[176] B. Han, C. Xu, *Int. J. Hydrogen Energy* **2014**, *39*, 18247.

[177] Y. Liu, C. Xu, *ChemSusChem* **2013**, *6*, 78.

[178] S. Li, X. Tang, H. Jia, H. Li, G. Xie, X. Liu, X. Lin, H.-J. Qiu, *J. Catal.* **2020**, *383*, 164.

[179] L.-M. Luo, W. Zhan, R.-H. Zhang, Q.-Y. Hu, Y.-F. Guo, X.-W. Zhou, *J. Catal.* **2020**, *381*, 316.

[180] J. Chen, Y. Li, N. Lu, C. Tian, Z. Han, L. Zhang, Y. Fang, B. Qian, X. Jiang, R. Cui, *J. Mater. Chem. A* **2018**, *6*, 23560.

[181] X. Wang, J. Sun, C. Zhang, T. Kou, Z. Zhang, *J. Phys. Chem. C* **2012**, *116*, 13271.

[182] S. Zaman, L. Huang, A. I. Douka, H. Yang, B. You, B. Y. Xia, *Angew. Chem. Int. Ed.* **2021**, *60*, 17832.

[183] Y. Ono, A. Ohma, K. Shinohara, K. Fushinobu, *J. Electrochem. Soc.* **2013**, *160*, F779.